CHAPTER 1

Water Desalination Revisited in Changing Physical and Economic Environments

YEHIA M. EL-SAYED*

*Dr. El-Sayed has regrettably passed away prior to the publication of this chapter. Final proofreading and some updating were done by the Editor. A tribute to his life was published as Testimonial, Yehia M. El-Sayed, *Energy* **36** 2315 (2011).

Advances in Water Desalination, First Edition. Edited by Noam Lior.

1.1 INTRODUCTION

The topic of water desalination is revisited because of the negative impact of the rising oil price index on the economic environment and the adverse effects of the increasing carbon footprint on the physical environment. In this introductory chapter, these negative factors are discussed with respect to their impact on past and present desalination methods. The impact of these factors on the design and operation practices of desalination and energy-intensive systems in general is highlighted. The energy analysis methodologies developed during the last two decades, including the methodology discussed in the present study, are summarized. General references on the subject matter are listed in the Further Reading section at the end of this chapter.

The software mentioned in this chapter may be downloaded at http://booksupport.wiley.com.

1.1.1 Past and Present Desalination

Interest in water desalination began in the late 1950s and early 1960s when the price of oil was only $3 per barrel (bl). A number of desalting processes and systems were considered that sought to minimize the cost of water production. For seawater, the leading methods were multistage flash distillation, vapor compression and freezing. Other processes, such as electrodialysis and reverse osmosis, lagged somewhat behind. Balancing the cost of the resources utilized in fueling a system and the resources utilized in making its devices favored moderate efficiency devices. For example, multistage flash distillation (MSF) in a cogeneration system

used a maximum temperature of around 190°F (~80°C) in 8–12 stages. Cost allocated to water was as low as $0.3/m^3$. Environmental constraints were virtually absent.

As the oil price index increased to $25/bl, the number of the stages of conventional MSF increased to about 20 and the cost allocated to water rose to about $1/m^3$. At the same time, the awareness and concern regarding increased CO_2 emissions also increased.

Present desalination methods are facing a continuing increase in oil prices and a continuing increase of CO_2 content in the air. This creates a serious concern to designers and operators of desalination plants, power plants, and energy-intensive plants in general. Innovative ideas, along with expanded R&D in certain directions, will be essential to boost prevailing technological advances to achieve higher-efficiency devices at lower cost.

Unfortunately, if the efficiencies of these devices are not high enough and their costs are not low enough, then promoting conservation may be necessary in order to reduce demand, followed by undesirable rationing.

1.1.2 The Emerged Concern

Early traditional approaches to the synthesis and design of energy-intensive systems relied on the intuition of experienced engineers and designers. Modest concern was given to fuel consumption, and no concern was given to the environment or to waste management.

The continuing rise in oil prices and the continuing increase in the carbon footprint did, indeed, create a concern. Today the concern is at its peak, fueled by an increase in world population looking for a higher standard of living.

The concern regarding the environment did rise to a global level and did pose a difficult challenge for the designers and operators of energy-intensive systems. Cost-effective fuel conservation became a focus of attention in the design and in the operation of these systems. The design aspects became a complex multidisciplinary process requiring specialized knowledge in each discipline. The operation aspects became more responsive to any missmanagement of energy, emissions, and waste disposal. Many research and development (R&D) projects emerged to target a new generation of energy systems to meet the challenge at both the producer end and the consumer end.

There was an increased demand for improved methods of system analysis to achieve lower cost and higher efficiency, to facilitate the work of system designers. The methods of improved energy analysis influenced the design and the manufacture of energy conversion devices. Devices are now designed for the system as a whole rather than being selected from lines of preexisting components. Manufacture models are developed for the devices to reduce overall cost. The low cost of "number crunching" has enhanced the development of energy-intensive analysis.

Almost all methods developed involve optimization and seek innovation through energy-intensive analysis. Common tools are modeling and computational algorithms. However, the tendency for models to involve assumptions and view the same system from different perspective has created variations in the quality and reliability of the developed models. It is, therefore, important that models be verified and also that both designers and operators be aware of the purpose of each model and its limitations.

1.1.3 The Emerged Energy Analysis Methodologies

The interaction between cost and efficiency has always been recognized qualitatively. However, the interest in formulating the interaction was first highlighted in connection with seawater distillation in the 1960s to gain insight into the interaction between the surface of separation requirement and energy requirement. The first landmark of the work on thermoeconomics [1] dealt with seawater desalination processes. Further development followed in 1970 [2,3]. Professor Tribus coined the word *thermoeconomics*. Professor Gaggioli [4,5] generated interest in extending the development to all kinds of energy-intensive systems.

Since then the interest spread nationally and internationally by a large number of investigators, and the development is still continuing. Various schools of thought regarding optimal system design have evolved in the last 30 years with the following common objectives:

- Increasing the ability to pinpoint and quantify energy inefficiencies.
- Providing further insight into possible improvements in system design and operation.
- Automation of certain aspects of the search for improvement.

Investigators differ with respect to the techniques of managing system complexity. Four techniques may be identified, all of which allow changes in system structure directly or indirectly:

- Construct an internal system economy as a system decomposition strategy. Most of the work by these techniques falls under the heading of either *thermoeconomics* or *exergoeconomics* [6–8].
- Consider a composite heat exchange profile of all heat exchange processes to identify where to add or reject heat and to produce and/or supply work appropriately. All work performed using this technique is termed “pinch technology” [9].
- Let the computer automate the analysis by supplying it with a large database of devices and their characteristics. All the work performed using this technique is classified as *expert systems* or *artificial intelligence* [10].
- Consider evolutionary techniques based on the survival-of-the-fittest theory [11,12] to identify the desired system.

The author recommended the references listed in Sections 1.F.1–1.F.7 at the end of this chapter as useful readings for the preceding material.

1.2 THE METHODOLOGY USED IN THIS STUDY

The methodology discussed in this chapter, termed *thermoeconomics*, begins with simple thermodynamic computations of a given system configuration on a trajectory leading to an optimal design via multidisciplinary computations involving the disciplines of design, manufacture, and economics, in addition to thermodynamics.

In a typical thermodynamic model, the cost factor is absent. Decision variables are mainly efficiency parameters of the processes involved, along with a few parameters such as pressure, temperature, and composition. The computations target fuel consumption, overall system efficiency, and duty parameters of the system devices. Evaluating cost involves input resources from the disciplines of design and manufacture in a prevailing economic environment. This, in turn, requires formulated communications among the participating disciplines.

Thermoeconomic analysis targets minimized production costs and is based on three main principles:

- Improved thermodynamic analysis, through the concept of exergy, to add transparency to the distribution of lost work (exergy destructions) throughout a system configuration.
- Improved costing analysis, by quantifying the manufacturing and operating costs of the devices of a system, to add transparency to the interaction between cost and efficiency.
- Enhanced optimization, via reasonable simplifying assumptions, to reach improved design points for alternative and evolving system configurations.

1.2.1 Improved Thermodynamic Analysis

Improved thermodynamic analysis extends the conventional thermodynamic computations to include the second law of thermodynamics *quantitatively* rather than *qualitatively*. The extended computations are simply entropy balance computations in addition to property computations and the conventional mass, energy, and momentum balances. Entropy is conserved in an ideal process and is created in a real process. The ideal adiabatic work of a compressor or a turbine (isentropic), for example, is obtained when the entropy remains constant. Actual adiabatic work is associated with entropy creation. The adiabatic efficiency relates the actual work to the ideal. The process inefficiency (irreversibility) measured as a lost work potential $= T_0\ S^c$, where T_0 is an ultimate sink temperature.

The main advantage of extended computations is that they enable assignment of fuel consumption to each process in a system. *Fuel* here means the input energy resource often applied at one location within the system boundaries. The energy resource may be fossil fuel, power, heat, solar, wind, or any other driving resource.

Thus, the manner in which a fuel is utilized throughout a system is revealed. Processes of high fuel consumption are identified. Means of fuel saving are inspired by a structural change of the system or/and by a design point change. New avenues of research and development are discovered.

It is important to note that engineers previously did not recognize the need to perform entropy balances. They could perform the thermodynamic analysis using property computations, and efficiency-related variables of a process such as pressure or heat loss, adiabatic efficiency, and heat exchange effectiveness. They missed the advantage of the distribution of fuel consumption throughout a given system.

A more complete picture of efficiencies and inefficiencies is obtained by using a general potential work function known as *exergy*. For simple chemical systems, this represents the maximum useful work relative to a dead-state environment defined by pressure P_0, temperature T_0, and composition $\{X_{c0}\}$. Exergy also represents the minimum amount of work needed to create the system from the dead-state environment.

1.2.1.1 The Exergy Function The exergy function is a general potential work function for simple chemical systems. The function evolved from the work of Carnot and Clausius, and is due to Gibbs [13]. The function is expressed as follows:

$$E^{s} = U + P_0 V - T_0 S - \sum \mu_{c0} N_c \tag{1.1}$$

Here, E^{s} is the maximum work that could be obtained from a sample of matter of energy U, volume V, number of moles (or mass) of each matter species N_c when the sample of matter is allowed to come to equilibrium with an environment of pressure P_0, temperature T_0, and chemical potential μ_{c0} for each species N_c. The same expression measures the least work required to create such a sample of matter from same environment. A form useful to second-law computations for systems in the steady state is

$$E^{f} = H - T_0 S - \sum \mu_{c0} N_i \tag{1.2a}$$

where E^{f} is flow exergy. For convenience, it is often expressed as the sum of two changes: (1) a change under constant composition $\{X_c\}$ from the state at P and T to a state at a reference point between P_0 and T_0 and (2) a change under constant P_0 and T_0 from composition $\{X_c\}$ to a state at reference $\{X_{c0}\}$. The state at $P_0 + T_0 + \{X_{c0}\}$ defines the reference dead-state environment for computing exergy

$$E^{f} = (H - H^{0}) - T_0 (S - S^{\circ}) + \sum (\mu_c - \mu_{c0}) N_c \tag{1.2b}$$

where $(H^{0} - T_0 S^{\circ})_{P_0, T_0, X_c} = (\sum \mu_c N_c)_{P_0 \cdot T_0}$ is used.

All special forms of potential workfunctions such as Carnot work, Keenam's availability, Helmholz free energy, and Gibbs free energy are obtainable from ideal interaction between a simple chemical system and large dead state environment using mass, energy and entropy balances as given by El-Sayed [14].

Section 1.A.3 (in the end-of-chapter Appendix) gives some useful forms of flow exergy in terms of measurable parameters and discusses the selection of the dead-state environment(s). Two or more dead-state environments may be used whenever there is no interest in their relative work potential. A known equilibrium chemical reaction may be introduced to establish the equivalent equilibrium composition of a missing species in a selected dead state environment.

1.2.2 Improved Costing Analysis

Most engineering activities seek the extreme of an objective function, which is usually a multicriterion function. Some criteria can be quantified in terms of monetary values such as fuel, equipment, and maintenance costs. Others involve nonunique assumptions regarding quantification of economic factors such as environmental impact, reliability, safety, and public health. In the design phase of an energy system, however, concern peaks around two criteria—*fuel* and *equipment*—without violating other desired criteria. A closer look at the interaction between fuel and equipment (products of specified materials and shapes) now follows to establish an improved costing analysis along with the improved thermodynamic analysis—in other words, to establish a thermoeconomic analysis.

Even when the objective function focuses on fuel and equipment only as costs, the analysis becomes multidisciplinary in nature. At least four disciplines of knowledge participate in information exchange: thermodynamics, design, manufacture, and economics. A communication protocol has to be established among the participating disciplines to provide cost with a rational basis.

Unfortunately, bidding information and some engineering practices for estimating the capital costs of major energy conversion devices are not helpful in the improvement of system design. The estimations are often oversimplified by a duty parameter for a group of devices such as a simple gas turbine unit costs of $500/kW. Such costs are not responsive to efficiency changes. The obvious way to recover missed information is to communicate with designers and manufacturers or to apply their practices encoded by suitable mathematical models.

1.2.2.1 The Quantification of the Manufacturing and Operation Resources for a Device Any energy conversion device requires two resources: those needed to manufacture it, R_{manuf}, and those needed to operate it R_{operate}. These two resources increase with the device duty (capacity and pressure–temperature severity) and are in conflict with the device performing efficiency (one or more efficiency parameters). Since both resources are expensive, their minimum sum is sought.

1.2.2.1.1 The Manufacturing Resources The leading manufacturing activities are materials, R&D, design, and construction. Exergy destruction associated

with the performed activities of these activities are difficult to trace back or evaluate. The capital cost of a device **Z** in monetary units is an indicator of the performed activities, if not the best indicator. The capital cost, in turn, may be expressed by one or more characterizing parameters and their unit-dimensional costs:

$$Z = \Sigma c_{ai} A_i + k \tag{1.3}$$

Usually one characterizing surface A_i of unit surface cost c_{ai} is an adequate quantification of Z. A_i is evaluated by an updated design model. The unit cost c_{ai} is a manufacturing cost evaluated by an updated manufacture model. The rate of the manufacturing resources then becomes

$$R_{\text{manuf}} = \mathbf{Z} = c_z c_{\text{a}}(V_{\text{manuf}}) A(V_{\text{design}}) \tag{1.4}$$

where **Z** is the capital cost rate and c_z is the capital recovery rate.

1.2.2.1.2 Operating Resources The primary operation resources are related to fueling and other maintenance materials and activities. The *fueling resource* is what the device pulls or draws from the fueling supply point. In other words, it is simply the *exergy destruction* performed by the device. Engineers, however, use efficiency parameters (pressure loss ratio, adiabatic efficiency, effectiveness, etc.) to account for exergy destruction. All devices destroy exergy for their operation, depending on their performance efficiency. Only ideal devices (operating at 100% efficiency), which do not exist, have zero exergy destruction when performing their duties. The rates of operating resources that do not go to the products are directly quantified by the rates of exergy destruction. In monetary units, the operating resources can be expressed as

$$R_{\text{operate}} = c_{\text{d}} D(\{V_{\text{duty}}\}, \{V_{\text{efficiency}}\}) \tag{1.5}$$

where D is the rate of exergy destruction of a device depending on its duty and efficiency and c_{d} is the cost of its exergy destruction; c_{d} depends on the cost of the fuel feeding the system and on the position of the device within the system configuration. The objective function J_i of a device i to minimize at the device level is

$$\begin{aligned} J_i &= R_{\text{manuf}} + R_{\text{operate}} \\ &= c_{zi} c_{ai}(V_{\text{manufacture}}) A_i(V_{\text{design}}) + c_{\text{di}} D_i(\{V_{\text{duty}}\}, \{V_{\text{efficiency}}\}) \end{aligned} \tag{1.6}$$

1.2.2.2 Correlating the Manufacturing Resources of a Device in Terms of Thermodynamic Variables Communication between the thermodynamic and the design models makes it possible to express A_i as a minimized surface $A_{i\,\min}(\{V_{\text{duty}}\}, \{V_{\text{efficiency}}\})$, and communication between the design and the manufacture models allows one to express $c_{ai} = Z_{\min}(V_{\text{manuf}})/A(V_{\text{design}})$ as a minimized unit surface price $c_{\text{a}\,\min}(\{V_{\text{duty}}\}, \{V_{\text{efficiency}}\})$.

State-of-the-art or updated design and manufacture models are sought for major system devices. A conventional thermodynamic model delivers to each device its respective $\{V_{\text{duty}}\}, \{V_{\text{efficiency}}\}$ obtained from one feasible system solution. The design model of the device minimizes the characterizing surface of the device by adjusting the design dimensions of the design model that represent its design degrees of freedom. The minimized surface $A_{\min}$ is sent to the manufacture model to minimize the manufacturing cost of the device design blueprint by adjusting the decision variables of the manufacture model, which represent its manufacturing degrees of freedom. The minimized unit surface cost $c_{\text{a min}}$ is the minimized manufacturing cost/$A_{\min}$.

This process is repeated over a range of feasible system solutions of interest to optimal system design. A matrix of rows representing feasible system solutions as related to a device and of columns representing thermodynamic duty and efficiency variables, design decision variables, and manufacture decision variables allows the manufacturing cost of a device in terms of design and manufacturing variables to be correlated in terms of thermodynamic variables.

A device objective function in terms of thermodynamic variables can be expressed as

$$\begin{aligned} J_i &= R_{\text{manuf}} + R_{\text{operate}} \\ &= c_z c_{ai\,\min}(\{V_{\text{duty}}\}, \{V_{\text{efficiency}}\}) A_{i\,\min}(\{V_{\text{duty}}\}, \{V_{\text{efficiency}}\}) \\ &\quad + c_{\text{di}} D_i(\{V_{\text{duty}}\}, \{V_{\text{efficiency}}\}) \end{aligned} \tag{1.7}$$

where $c_{ai\text{mn}}, A_{i\,\min}$, and D_i are all functions of $\{V_{\text{duty}}\}$ and $\{V_{\text{efficiency}}\}$, tending, in general, to increase with duty, and are at conflict with efficiency.

Communication between the system thermodynamic model and the design models of its devices has been applied to a fair number of any conversion devices as given in Section 1.A.1. An example of such communication for forced-convection heat exchangers, in which the manufacturing cost of a heat exchanger is expressed in terms of thermodynamic variables, is given in Section 1.A.2.

However, the communication between design and manufacture is still lagging. The unit surface manufacture cost is derived, at the moment, from published cost information rather than by manufacturing models. The communication between design and manufacture models of devices is still being formulated.

1.2.3 Enhanced Optimization

1.2.3.1 Two Simplifying Assumptions The optimization of an energy system configuration is most expedient when the system devices are optimized one by one with respect to the decision variables of the system. Improved thermodynamic and costing analyses have two basic features that qualify a system for device-by-device optimization:

- The assignment of fuel consumption to each device of the system establishes the operating costs of the system devices.

- Most of the decision variables are efficiency parameters whose major impact is on the local manufacturing costs of their respective devices.

Two simplifying assumptions are introduced to allow device-by-device optimization with respect to efficiency decisions as explained in the following paragraphs:

- An average exergy destruction cost applies to all devices.
- Efficiency decisions are local to their devices followed by a correction for their effect on other devices.

1.2.3.2 The Conditions of Device-by-Device Optimization The objective function of a device is expressed in Equation (1.7). The objective function of a system configuration, in terms of $\{V_{\text{duty}}, V_{\text{efficiency}}\}$, given a sizing parameter for the production rate and having one fueling resource, is

$$\begin{aligned}\text{Minimize } J_s &= c_F F + \sum_{i=1}^{n} \underline{Z_T} + C_R \\ &= c_F F + \sum_{i=1}^{n} \underline{Z_i} + C_R \\ &= c_F F + \sum_{i=1}^{n} C_{zi} Z_i + C_R \\ &= c_F F(\{V_{duty}, V_{efficiency}\}) + \sum_{i=1}^{n} c_{zi} c_{ai} A_i(\{V_{duty}, V_{efficiency}\}) + C_R \end{aligned} \quad (1.8)$$

where F is fuel rate; $\underline{\mathbf{Z}_{\mathrm{T}}}$ the total capital cost recovery rate; $\underline{\mathbf{Z}_i}$ the capital cost recovery rate of a device; n, the number of devices; and Z_i, the capital cost of each device represented by one characterizing dimension A_i. C_{R} is a constant remainder cost as far as the system design is concerned. When a design becomes a project, C_{R} may become a variable with respect to other non-system-design decisions.

To express the cost objective function of a system [Eq. (1.8)] in terms of the functions of the manufacturing and operating resources of its devices [Eq. (1.7)], the following condition must apply to a device i after dropping the constant C_{R}:

$$\frac{\partial J_{\mathrm{s}}}{\partial Y_j} = \frac{\partial J_i}{\partial Y_j} = 0 \quad (1.9)$$

where Y_j is a system decision variable, J_{s} is the objective function of the system, and J_i is that function of a device i in the system:

$$\begin{aligned}\frac{\partial J_{\mathrm{s}}}{\partial Y_{\mathrm{j}}} &= c_{\mathrm{f}} \left(\frac{\partial E_{\mathrm{F}}}{\partial D_i}\right)\left(\frac{\partial D_i}{\partial Y_j}\right) + \left(\frac{\partial Z_{\mathrm{T}}}{\partial Z_i}\right)\left(\frac{\partial Z_i}{\partial Y_j}\right) = c_{\mathrm{f}} \mathrm{K}_{e\,\mathrm{ji}} \frac{\partial D_i}{\partial Y_j} + K_{zji}\left(\frac{\partial Z_i}{\partial Y_j}\right) \\ &= \frac{\partial J_i}{\partial Y_j} \end{aligned} \quad (1.10)$$

where

$$c_{\mathrm{F}}F = c_{\mathrm{f}}E_{\mathrm{F}} \tag{1.11a}$$

$$K_{\mathrm{e}ji} = \left(\frac{\partial E_{\mathrm{F}}}{\partial D_i}\right) \text{by a small change in } Y_j \tag{1.11b}$$

$$K_{zji} = \left(\frac{\partial Z_{\mathrm{T}}}{\partial Z_i}\right) \text{by a small change in } Y_j \tag{1.11c}$$

IF $K_{\mathrm{e}ji}$ and K_{zji} are independent of Y_j or at least weak functions of Y_j, then Equation (1.9) gives the objective function of a device as follows:

$$J_i = c_{\mathrm{f}}K_{\mathrm{e}ji}D_i + K_{zji}Z_i \tag{1.12a}$$

$$= c_{\mathrm{d}\,i}D_i + c_{zi}c_{a\mathrm{i}}A_i \tag{1.12b}$$

Then $c_{\mathrm{d}\,i} = c_{\mathrm{f}}K_{eji}$, and the capital cost rate is modified by K_{zji}.

The condition that a device can be self-optimized in conformity with the objective function of its system is that $K_{\mathrm{e}ji}$ and K_{zji} can be treated as constants.

The major effects of most efficiency decision variables on their respective devices ($K_{\mathrm{e}ji} = K_{e\,\mathrm{ii}}$), converging to the condition of Equation (1.9) with $K_{zii} = 1$. They are denoted as local Y_{L}. Few efficiency decisions have their major effect on more than one device such as heat exchange effectiveness of two heat exchangers in series. These are identified as global Y_{G}. Their values {$K_{\mathrm{e}ji}$ and K_{zji}} will continue to change, leading to random fluctuations of the system objective function with no sign of convergence. A slower optimization routine, often gradient-based, has to be used for these few global decisions. Because most efficiency decision variables are designated as local, it is worthwhile to utilize the piecewise optimization of the system devices, to gain insight into possible improvements and to ensure rapid optimization.

1.2.3.3 The Form of $A_{i\,\mathrm{min}}$ and D_i of a Device A suitable form to express $A_{i\,\mathrm{min}}$ and D_i in terms {$V_{i\,\mathrm{duty}}$} and {$V_{i\,\mathrm{efficiency}}$}, particularly for optimization, is a form extracted from geometric programming:

$$A_{i\,\mathrm{min}} = k_a \prod_{j=1}^{n} (V_{i\,duty})_j^{d_a} (V_{i\,\mathrm{efficiency}})_j^{e_a} \tag{1.13}$$

$$D_i = k_d \prod_{j=1}^{n} (V_{i\,\mathrm{duty}})_j^{d_d} (V_{i\,efficiency})_j^{e_d} \tag{1.14}$$

where k_{a} and k_{d} are constants; n is the number of correlating variables, and d_{a}, e_{a}, d_{d}, and e_{d} are exponents. For the local decisions

$$J_i = c_{\mathrm{f}}K_{\mathrm{e}i}D_i(Y_{\mathrm{L}i}) + K_{\mathrm{z}i}c_{\mathrm{z}i}c_{\mathrm{a}i}A_i(Y_{\mathrm{L}i}) \tag{1.15}$$

where the exergy destruction price $c_{\mathrm{d}\,i} = c_{\mathrm{f}} K_{\mathrm{e}\,i}$ and $K_{\mathrm{e}i} = \delta E_{\mathrm{F}}/\delta D_i$ through a change δY_{Li} and is always a positive quantity. $K_{\mathrm{e}\,i}$ converges to a constant, and K^{zi} converges to 1.

Equation (1.15) boils down, as far as the optimization of $Y_{L\mathrm{i}}$ is concerned, to a generalized form of a Kelvin optimality equation:

$$J_i = k_{\mathrm{e}} Y_{\mathrm{L}\,i}{}^{\mathrm{ne}} + k_z Y_{Li}{}^{nz} \tag{1.16}$$

where k_e and k_z are lumped energy and the capital factors, considered weak functions of Y_{Li}, and n_{e} and n_{z} are exponents of opposite signs. The Kelvin optimality equation has the exponents 1 and -1. If k_{e} and k_{z} were precisely constants, then the optimum is reached in one system computation by the analytical solution

$$Y_{\mathrm{L}\,i\,\mathrm{opt}} = \left[\frac{-(k_z n_z)}{(k_{\mathrm{e}} n_{\mathrm{e}})}\right]^{1/(n_{\mathrm{e}} - n_z)} \tag{1.17}$$

1.2.3.4 Convergence to System Optimum The decisions idealized as local are not in complete isolation from the rest of the system. They influence the duties passed over from their devices, as mass rates, heat rates, or power, to other devices. The effect of these duties on cost within the range of system optimization is linear. To allow for this mild variation to adjust and converge to the system optimum, system computations are repeated using the analytical solutions of Equation (1.17) as an updating equation.

Substituting D_i and A_i for k_{e} and k_z, we obtain the updating equation for convergence:

$$Y_{\mathrm{L}\,i\,\mathrm{new}} = Y_{\mathrm{L}i\,\mathrm{old}} \left[\frac{(-n_{\mathrm{m}}/n_{\mathrm{e}})(c_{zi} c_{\mathrm{a}i} A_i)}{c_{\mathrm{d}\,i} D_i}\right]^{1/(n_{\mathrm{e}} - n_{\mathrm{m}})} \tag{1.18}$$

Equation (1.18) happens to converge to a system's optimum in seconds (four to six iterations).

1.2.3.5 Optimization of System Devices by One Average Exergy Destruction Price According to Equation (1.15), each device i has its own exergy destruction price $c_{\mathrm{d}\,i}$. With K_{zi} converging to 1, we obtain

$$\sum c_{\mathrm{d}\,i} D_i = c_{\mathrm{f}} E_{\mathrm{f}} = c_{\mathrm{f}} \left(\sum D_i + \sum D_j + \sum E_{\mathrm{p}}\right) \tag{1.19}$$

where $\{E_{\mathrm{p}}, E_{\mathrm{f}}\}$ are exergies of feeds and products, $\{D\}$ are exergy destruction by the devices, and $\{E_j\}$ exergy of wasted streams and $\mathrm{c_f}$ is fuel price per unit exergy. Then, introducting an average c_{da} such that

$$c_{\mathrm{da}} \sum D_i = \sum c_{\mathrm{d}\,i} D_i = c_{\mathrm{f}} E_{\mathrm{f}} = c_{\mathrm{f}} \left(\sum D_i + \sum D_j + \sum E_{\mathrm{p}}\right)$$

we obtain

$$c_{da} = c_f(1 + \sum D_j / \sum D_i + \sum E_p / \sum D_i) \tag{1.20}$$

A slightly higher c_d than c_{da} often improves further the desired objective function.

1.2.3.6 Global Decision Variables Few decision variables belong to the system as a whole and are considered global. Operating pressure and temperature levels of a system are examples of global decisions. Occasionally a local decision such as a temperature difference has a global effect. Devices are not decomposed with respect to these decisions. A nonlinear programming algorithm may be invoked to solve for the optimum of these decisions simultaneously. If the range of variation of global decisions is narrow, manual search may be sufficient. For automated optimization, a simplified gradient-based method that ignores cross second derivatives may also be sufficient. This simplified method avoids singular matrices, which block solutions and often occur in systems of process-oriented description. It also converges, if guided to differentiate between a maximum and a minimum, as shown by the following updating equations for a global decision Y_G:

$$Y_{G\,\text{new}} = Y_{G\,\text{old}} \pm \Delta Y \tag{1.21a}$$

$$\Delta Y = \text{ABS}\left[\frac{\delta Y}{(g_2 - g_1)(-g_1)}\right] \tag{1.21b}$$

$$g_1 = \frac{(J_1 - J_0)}{\delta Y} \tag{1.21c}$$

$$g_2 = \frac{(J_2 - J_1)}{\delta Y} \tag{1.21d}$$

$$\delta Y = Y_{G1} - Y_{G0} = Y_{G2} - Y_{G1} \tag{1.21e}$$

The updating equation [Eq. (1.21)] requires three system computations to obtain three neighboring values of the objective function assuming, for example, Y_{G0}, $Y_{G0} + \delta Y$ and $Y_{GO} + 2\delta Y$ for each global decision. After $\{\Delta Y\}$ of the simultaneous solution has been obtained, the $\pm$ sign is then assigned to guide the change in the favored direction because zero gradient represents both maximum and minimum.

References listed in Section 1.F.8 at the end of this chapter are additional useful readings for the preceding Section 1.2.

1.3 THE SCOPE OF ANALYSIS

1.3.1 Desalination Related to Physical and Economic Environments

Desalted water is either coproduced with power production where the combined system is fossil-fuel-driven or self-produced, driven indirectly by fossil fuel by engines or by power from the grid. Most grid power is fossil-fuel-driven. The remaining grid power is driven by renewable sources of energy or by nuclear energy.

When desalted water is fossil-fuel-driven, two streams are to be dumped in the environment: an exhaust gas stream and a concentrated brine stream. When the exhaust is dumped in air CO_2 emission occurs. When concentrated brine is dumped back into the sea, marine life is damaged; and when dumped underground, the salinity of the underground water rises fast because of the limited amount of underground water. Dumping waste directly in the physical environment is the cheapest way to dispose of waste, but at the expense of the environment.

When desalted water is driven by solar, wind, or tidal energy, only the brine stream needs to be dumped. Exhaust gases are absent as well as CO_2 emission. Thus, in terms of CO_2 emission, renewable-energy-driven desalination systems are the most ecofriendly.[1]

For fossil-fuel-driven desalination systems, the higher the efficiency of the system, the lower the fuel burning and hence the CO_2 emission for the same produced product(s). This pattern continues until cost loses its competitiveness in the market as a limit to the reduction of CO_2 emission. The economic environment imposes the limit.

In view of the points discussed above, a number of desalination systems will be evaluated in terms of efficiency, cost, and CO_2 emission, assuming that direct dumping of concentrated brine is tolerated.

The avoidance of direct brine dumping will be treated by going to zero liquid discharge where more desalted water is obtained and solid salts can be safely transported isolated dumping locations. Predumping treatment is another option to safe dumping but is not considered in this study.

The idea of generating power by the concentration difference between concentrated brine and seawater will be investigated as a source of power though it does avoid the effect of direct dumping.

1.3.2 The Systems Considered

Systems with nine different configuration types, each intended for a specified purposes, are considered here. Four configuration types are fossil-fuel-driven burning natural gas, two are grid-power-driven, two are solar-driven, and one is concentrated-brine-driven. The purpose is to capture ideas that may help meet the challenges of diminishing fossil-fuel resources, increased CO_2 emissions, and hazardous-waste dumping.

The methodology of analysis is explained in Section 1.2. Accordingly, each system is described with respect to its working fluids and their thermodynamic properties and by its devices and their thermodynamic decision variables. The decision variables are used to solve mass balance, energy balance, and exergy

[1]More accurate assessment of energy and environmental impact should include calculation of embodied energy and emissions, i.e. the energy and emissions associated with the system construction. These might be rather high when renewable energy such as solar, wind, marine or osmotic is used, because of the relatively large quantity of hardware needed. These were not included in this chapter, which does not diminish the value of its conclusions, especially since embodied values are often small relative to operational ones. The Editor-in Chief.

balance equations leading to a feasible solution with the lower number of iterative loops. A characterizing surface of heat transfer, mass transfer, or momentum transfer is identified for each device. The cost of the device is rated per unit manufacturing cost of the characterizing surface. Decision variables are changed manually to minimize a cost objective function of the system.

The flow diagrams of the systems considered for their purposes are Figures 1.1–1.9. Figure 1.1 shows the gas turbine/multistage flash distillation (GT/MSF) cogeneration system with 100 MW power. Figure 1.2 shows the simple combined cycle (SCC) at 100 MW power, with compressor pressure 135 psia and firing temperature 1600°F. Figure 1.3 shows the vapor compression (VC) system of 10 migd (million imperial gallons per day) water. Figure 1.4 shows VC at the same capacity but with zero liquid discharge. Figure 1.5 depicts the reverse-osmosis (RO) system in one and two stages of 10 migd water. The two-stage system is a standby system in case one stage fails to deliver potable product water. Figure 1.6 shows an RO of the same capacity but for zero liquid

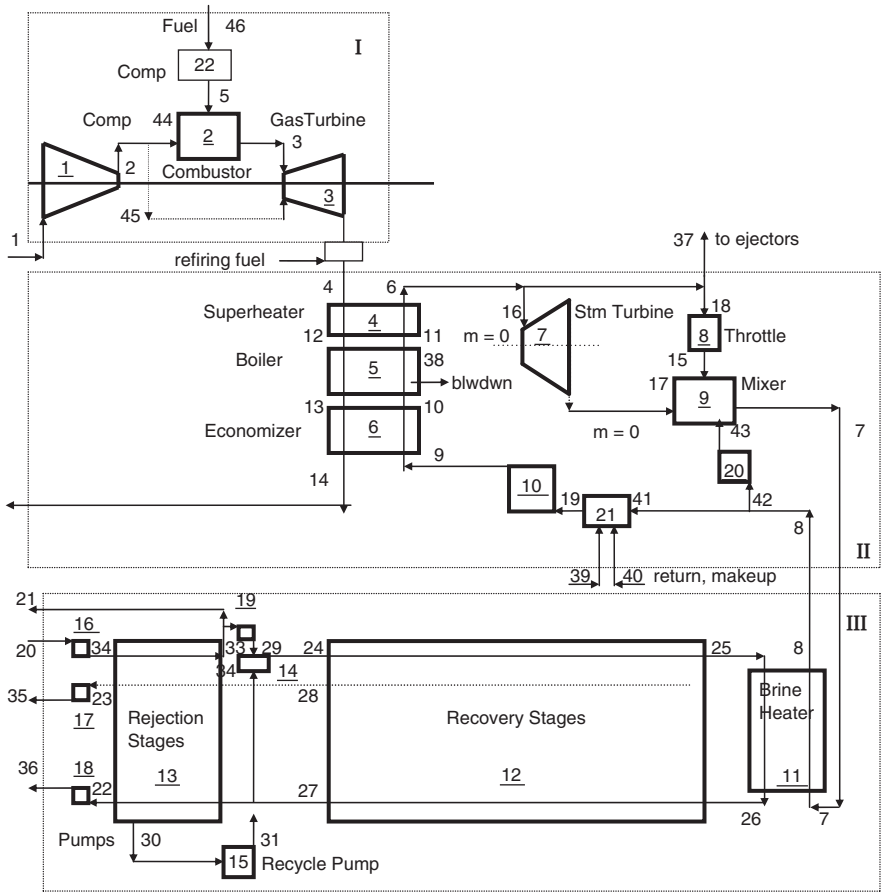

Figure 1.1 Gas turbine/multistage flash distillation cogeneration system.

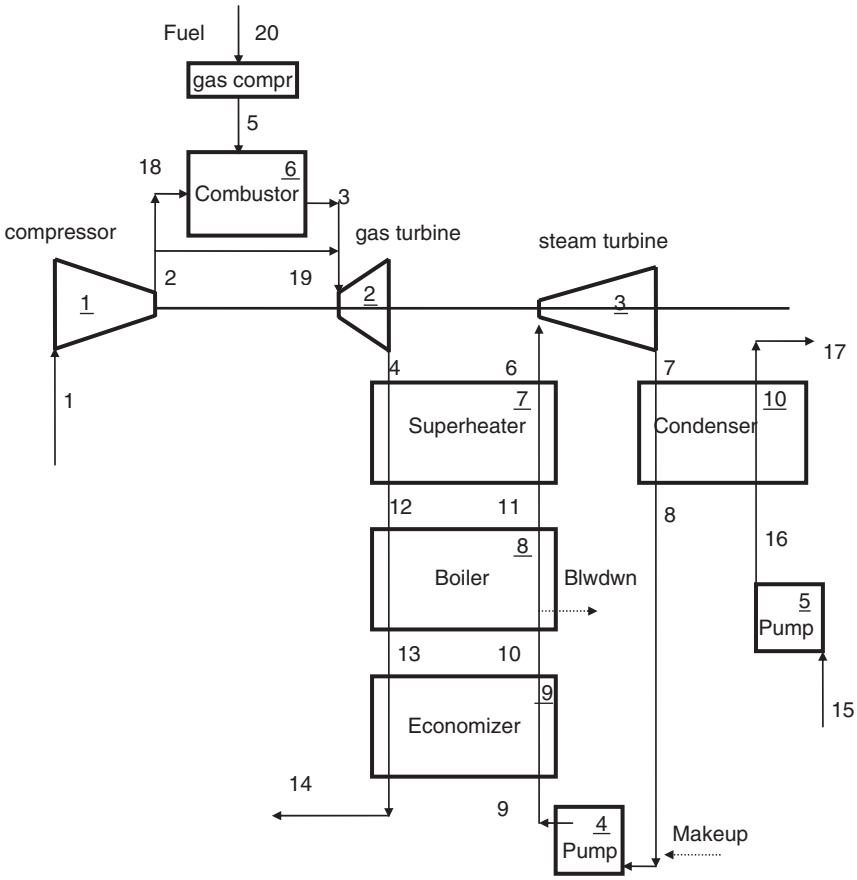

Figure 1.2 Simple combined cycle SCC.

discharge. Figure 1.7 shows a 0.2-usmgd solar photovoltaic/reverse-osmosis (PV/RO) system for small communities of about 1000 people. Figure 1.8 shows a 1-usmgd solar photovoltaic/electrodialysis (PV/ED) system for partial recovery of irrigation drainage. Figure 1.9 represents a concentrated-brine-driven system for power generation Delta-Xs-Power (osmosis power). A concentrated brine stream of 10 usmgd is assumed.

For the systems in Figures 1.1–1.6, the imperial gallon was used. For the systems in Figures 1.7–1.9, the us gallon was used. (The imperial gallon is 1.2 US gallons.)

For the systems in Figures 1.1–1.3, the optimization is automated for the efficiency decision variables. The design models of the devices of these systems have many design degrees of freedom to generate preformulated design-based costing equations for the devices. This, in turn, allows for automated computation of the minimized characterizing surfaces. Minimization of the cost objective functions the devices is enhanced given the unit surface costs and the unit exergy destruction costs of the devices.

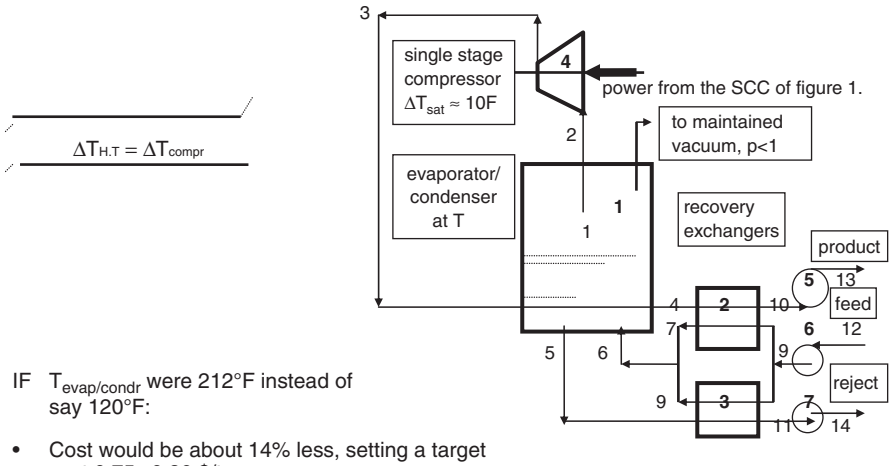

IF $T_{evap/condr}$ were 212°F instead of say 120°F:

- Cost would be about 14% less, setting a target cost 0.75–0.80 $/ton
  Compressor Capacity would increase 15 times.
- Venting substitutes vacuum.

Figure 1.3 Vapor compression distiller VC.

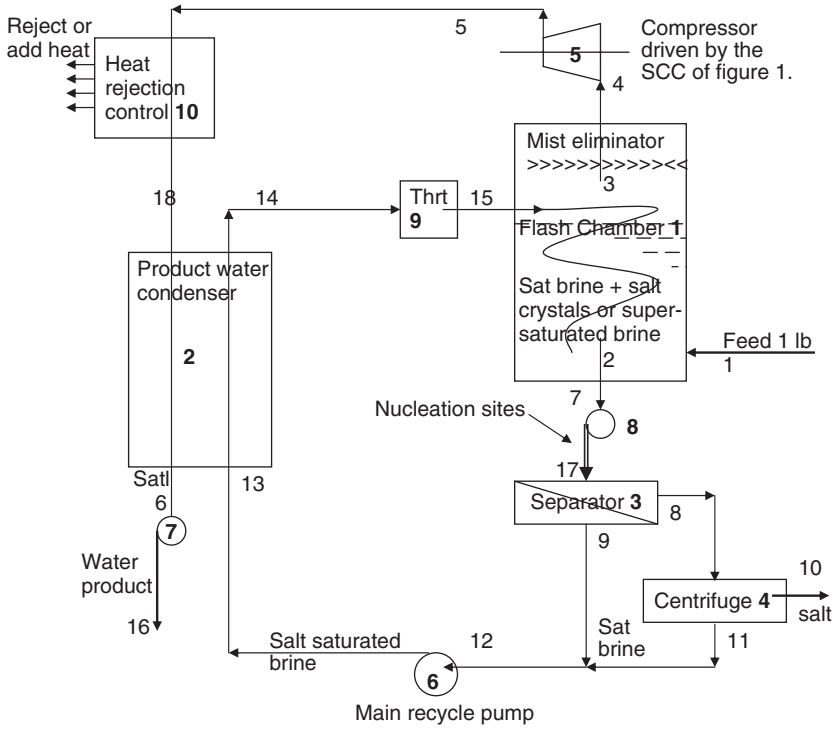

Figure 1.4 Vapor compression distillation system with zero liquid discharge.

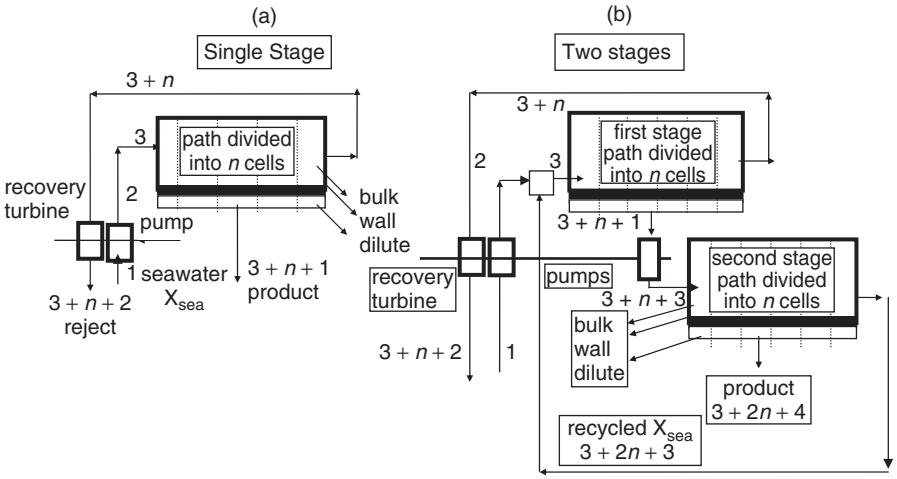

Figure 1.5 Reverse-osmosis desalting system RO: (a) single-stage; (b) two-stage.

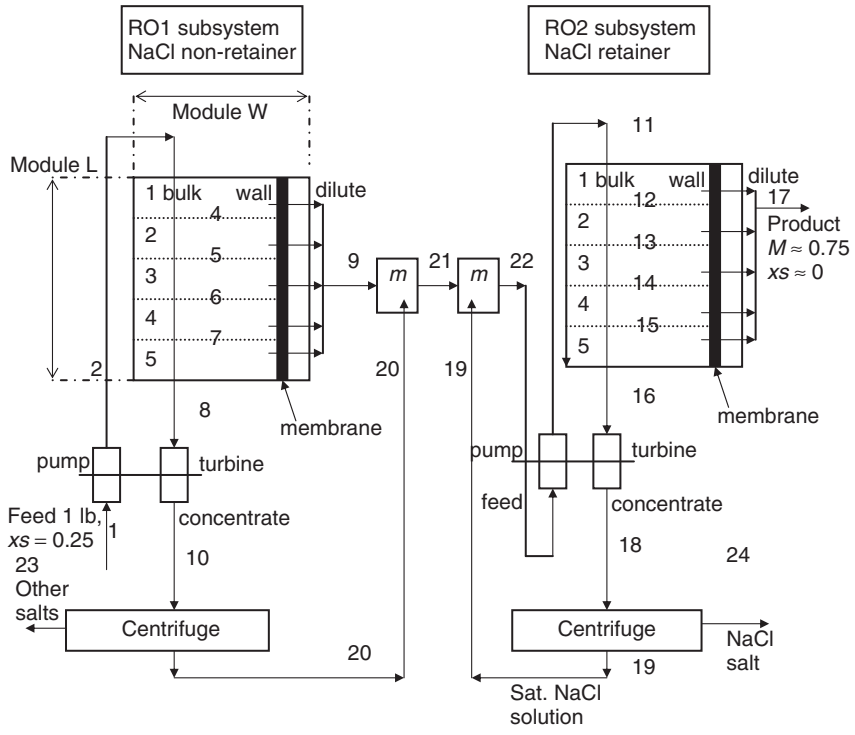

Figure 1.6 Reverse osmosis with zero liquid discharge.

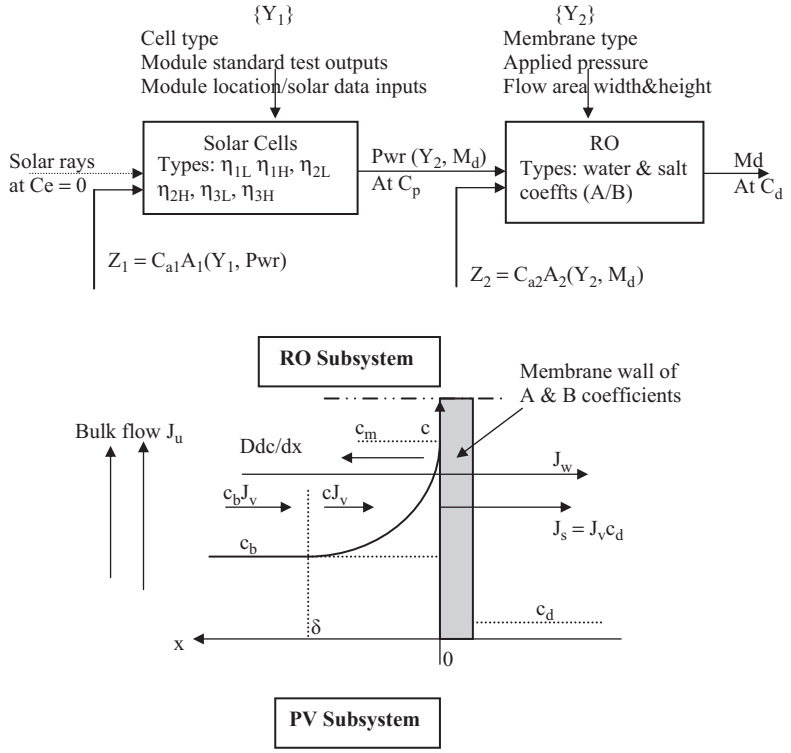

Type	Lower η°		Higher η°	
	η	$/pW	η	$/pW
1) Amorphous Silicon (a-Si:H):	6%	3.4	15%	1.7
2) Czochralski (Cz-Si):	12%	4.6	17%	3.4
3) Multi-junction, 500X concentrator	17%	2.9	22%	2.4

Figure 1.7 The Photovoltaic/Reverse osmosis desalination system PV/RO.

For the remaining systems the optimization is manual since there are not enough design options (design degrees of freedom), unlike those of the devices of systems 1–3.

Each system has two design points: a reference design point and an improved design point, by automated or manual optimization. Two economic environments are also considered. One represents an oil price index of $25/bl (barrel) and the other one represents $100/bl. Although it is difficult to predict the price structure under rising oil prices, a simple prediction is assumed. Fuel, power, and steam costs at a rate of 100/bl are set at 4 times those at $25/bl. Capital cost of devices and the cost products are set at a lower rate of 2 times.

The GT/MSF system is designed for two products (power and water) while being driven by a single fuel resource. Often, the decision variables of the system permit one product rate as a decision variable. A power of 100 MW is selected as

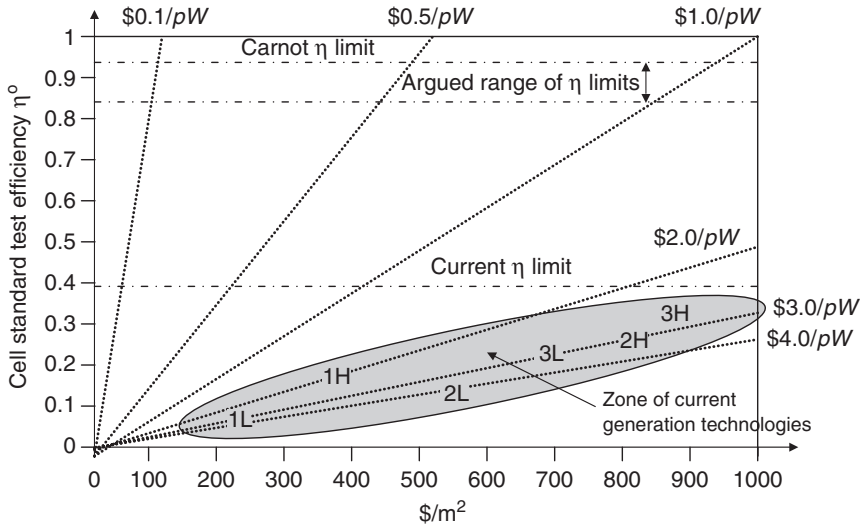

Figure 1.8 Current competitiveness of PV/RO system [18]. pW: peak watts.

the decision product rate. The objective of maximizing profitability is considered for this particular system, in which computed water product rates ranged from 8 to 10 migd.

For cogeneration systems such as the GT/MSF system, various assumptions have been proposed to allocate the production cost to water and power. The assumptions are all logical but the allocations differ significantly. The allocation assumed here uses the capital cost of each subsystem as belonging to that subsystem. The fuel is allocated in proportion to the exergy destructions and waste streams of each subsystem. This gives a lower bound to the cost of water since no devices or their exergy destructions are shared by the two subsystems. Higher water cost is obtained if the exergy destruction of combustion is shared.

For the GT/MSF and SCC systems a default power load profile that varies from 20 to 100 MW with a load factor of 0.583 is assumed. Both ideal and actual control features are considered. Ideal control assumes design efficiency at all load fractions (implying variable geometry devices). The actual control considered keeps the rate of airflow to the gas turbine compressor at the design value while increasing the air/fuel ratio. A quadratic equation for system efficiency as function of load fraction is assumed for design efficiency at maximum load and 20% efficiency at minimum load. Both GT/MSF and SCC systems are run without and with night products to evaluate the effects of improved load factor. Both systems considered include an RO subsystem for the night product. Two time periods are identified. The first lasts from midnight to 6 A.M. where a power of 80 ± 0.5 MW is available. The second lasts from 7 P.M. to 11 P.M. where a power of 40 MW ± 0.5 MW is available. For the SCC system, a water electrolysis subsystem producing H_2 and O_2 as night products is also considered.

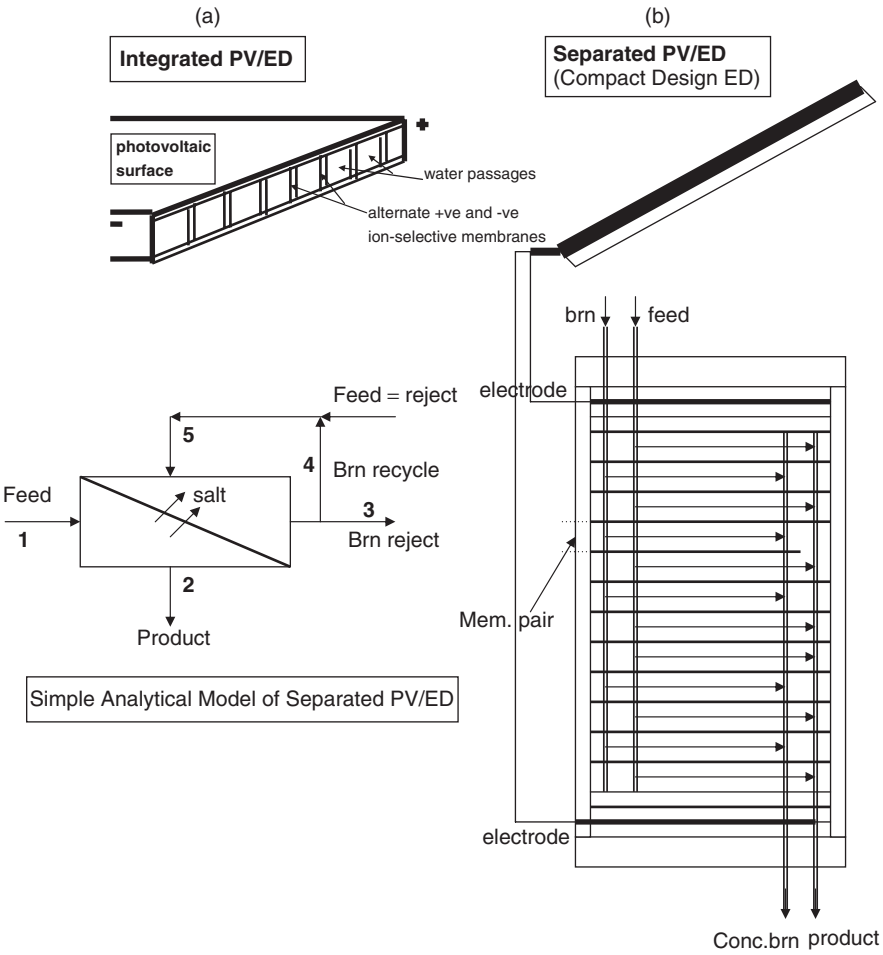

Figure 1.9 Photovoltaic/electrodialysis (PV/ED) system: (a) integrated PV/ED; (b) separated PV/ED (compact design ED).

For the SCC-driven VC and RO desalting systems, two types of rejected stream disposal are assumed: a conventional brine discharge and a salt discharge (zero liquid discharge).

For the PV/RO and PV/ED solar systems, a solar intensity profile at 30° north latitude is assumed.

For the Δ-X_{salt}-Power system (osmosis power), sodium chloride ideal solution is assumed. Salt content 0.04 is assumed for sea and $\leq$ 0.25 salt content is assumed for the driving brine.

Sample runs of the various systems considered are given in Tables 1.1–1.7. Table 1.1 lists data obtained for GT/MSF cogeneration runs; Table 1.2, SCC power runs; Table 1.3, SCC/VC runs; Table 1.4, SCC/RO runs; Table 1.5, PV/RO runs; Table 1.6, PV/ED runs; Table 1.7, osmosis power of Δ-X_{salt}.

Table 1.1 Gas Turbine/Multistage Flash Distillation Systems

	Reference System						Improved by Higher Profitability					
	Design Steady-Load Operation		Variable Load Operation No 2nd Product		Night RO Desalter Operation		Design Steady-Load Operation		Variable Load Operation No 2nd Product		Night RO Desalter Operation	
	Oil Index, $		Oil Index, $		Oil Index, $		Oil Index, $		Oil Index, $		Oil Index, $	
Parameter	25	100	25	100	25	100	25	100	25	100	25	100
Power, MW	100	100	58.3	58.3	86.5	86.5	100	100	58.3	58.3	99	99
Water, migd	8.04	8.04	8.04	8.04	8.04	8.04	10.1	9.25	10.1	9.25	10.1	9.25
Water, t/h	1,496	1,496	1,496	1,496	1,496	1,496	1,871	1,721	1,871	1,721	1,871	1,721
Fuel, MWt	350	350	224	224	308	308	338	306	216	194	297	266
To water	64.9	64.9	41.7	41.7	57.2	57.2	66.8	55	43	33	59	46
To power	285	285	183	183	251	251	271	251	173	161	238	221
1st law eff	0.301	0.301	0.266	0.266	0.326	0.326	0.313	0.334	0.276	0.303	0.338	0.375
2nd law eff	0.355	0.355	0.289	0.289	0.355	0.355	0.365	0.391	0.295	0.329	0.368	0.405
CO_2, t/h	64.1	64.1	63.8	63.8	64	64	62	56.1	61.6	55.8	61.8	56
To water	11.9	11.9	11.8	11.8	11.9	11.9	12	10	12.2	10	12.2	10
To power	52.2	52.2	51.9	51.9	52.1	52.1	50	46	49.4	45.8	49.6	46
lb/lb fuel	2.6	2.6	4.04	4.04	2.9	2.9	2.6	2.6	4.04	4.07	2.95	2.98
lb/kWhe	1.14	1.14	1.96	1.96	1.33	1.33	1.1	1.01	1.86	1.73	1.1	1.02
lb/tn water	17.5	17.5	17.4	17.4	17.5	17.5	14.1	12.8	14.3	12.8	14.3	12.8
Capital, $M	154	308	154	308	154+	308+	191	410	191	410	191+	410+
Capital, $/h	1,925	3,854	1,925	3,854	1,925+	3,854+	2,388	5,125	2,388	5,125	2,388+	5,125+
Fuel, $/h	3,497	13,987	2,196	8,785	3,013	12,125	3,379	12,247	2,115	7,694	2,924	10,620
Production, $/h	5,424	17,840	4,171	12,830	5,593	17,562	5,764	17,366	4,547	12,981	6,052	16,599

(*Continued*)

Table 1.1 (***Continued***)

	Reference System						Improved by Higher Profitability					
	Design Steady-Load Operation		Variable Load Operation No 2nd Product		Night RO Desalter Operation		Design Steady-Load Operation		Variable Load Operation No 2nd Product		Night RO Desalter Operation	
	Oil Index, $		Oil Index, $		Oil Index, $		Oil Index, $		Oil Index, $		Oil Index, $	
Parameter	25	100	25	100	25	100	25	100	25	100	25	100
Revenue, $/h	6,687	24,965	4,570	15,556	11,882	30,181	7,199	25,538	5,065	16,142	12,377	30,767
Profit, $/h	1,263	7,124	399	2,726	6,180	12,619	1,434	8,172	518	3,162	6,325	14,169
Design case allocation												
C_{wtr}, $/t	1.02	2.91	0.859	2.264	0.96	2.678	1.058	2.88	0.925	2.558	1.01	2.987
C_{pwr}, $/kWh	0.038	0.134	0.048	0.158	0.04	0.138	0.037	0.123	0.047	0.143	0.039	0.123
C_{da}, $/kWh	0.023	0.091					0.035	0.12				
Some decisions												
MSF stages	18	18	18	18	18	18	22	28	22	28	22	28
Pinch	50	50	50	50	50	50	9	11	9	11	9	11
Efficiency levels	0.85	0.85	9.85	0.85	0.85	0.85	0.9	0.92	0.9	0.92	0.9	0.92
Op_{pen} MW	—	—	26.1	26.1	8.04	8.04	—	—	25.1	22.8	7.7	7.05
$/h	—	—	260	1,042	80	320	—	—	251	913	77	281
Cap+, $/h	—	—	—	—	696	1,392	—	—	—	—	696	1,392
Prd+, t/h	—	—	—	—	5,625	5,625	—	—	—	—	5,625	5,625

Table 1.2 Combined Cycle Power Systems

	Reference System						Improved by Lower Production Cost					
	Design Steady-Load Operation		Variable Load Operation, No 2nd Product		Night Operation of RO and EL		Design Steady-Load Operation		Variable Load Operation, No 2nd Product		Night Operation of RO and EL	
	Oil Index, $		Oil Index, $		Oil Index, $		Oil Index, $		Oil Index, $		Oil Index, $	
Parameter	25	100	25	100	25	100	25	100	25	100	25	100
Power, MW	100	100	58.3	58.3	86.5	86.5	100	100	58.3	58.3	86.5	86.5
Fuel, MW	248.5	248.5	164.5	164.5	220.9	220.9	246.8	227.4	163.3	150.5	219.3	202.1
CO_2, t/h	45.5	45.5	28.9	28.9	39.7	39.7	45.2	41.7	28.7	26.5	39.4	36.3
lb/lb fuel	2.7	2.7	2.6	2.6	2.65	2.65	2.7	2.7	2.6	2.59	2.65	2.64
lb/kWhe	1.002	1.002	1.09	1.09	1.01	1.01	0.99	0.916	1.08	0.948	1.002	0.924
1ST law Efficiency	0.402	0.402	0.355	0.355	0.391	0.391		0.44	0.357	0.388	0.394	0.428
2nd law Efficiency	0.461	0.461	0.385	0.385	0.425	0.425		0.51	0.388	0.421	0.428	0.465
Capital, $M	92.3	184.7	92.3	184.7	92.3+	184.7+	82	189.4	82	189.4	82+	189.4+
Capital, $/h	1,155	2,310	1,155	2,310	1,155+	2,310+	1,032	2,369	1,023	2,369	1,023+	2,369+
Fuel, $/h	2,485	9,943	1,645	6,581	2,209	8,837	2,468	9,096	1,633	6,021	2,193	8,085
Production, $/h	3,641	12,253	2,800	8,891			3,500	11,465	2,656	8,390		
Revenue, $/h	4,500	20,000	2,625	11,667			4,500	20,000	2,625	11,667		
Profit, $/h	859	7,747	−175	2,776			1,000	8,535	−31	3,277		
Operation												
F_{pen} MW			19.5	19.5	6.03	6.03			19.3	17.8	5.98	5.5
F_{pen}, $/h			195	781	60	241			193	714	59	220
RO at night												
Production, $/h					4,060	12,542					3,922	11,150
Revenue, $/h					9,938	26,292					9,938	26,292

(*Continued*)

Table 1.2 (*Continued*)

	Reference System						Improved by Lower Production Cost					
	Design Steady-Load Operation		Variable Load Operation, No 2nd Product		Night Operation of RO and EL		Design Steady-Load Operation		Variable Load Operation, No 2nd Product		Night Operation of RO and EL	
	Oil Index, $		Oil Index, $		Oil Index, $		Oil Index, $		Oil Index, $		Oil Index, $	
Parameter	25	100	25	100	25	100	25	100	25	100	25	100
Profit, $/h					5,877	13,752					6,016	15,142
NightCap, $/h					696	1,392					696	1,392
Production, t/h					5,625	5,625					5,625	5,625
C_{prd}, $/t					0.24	0.74					0.24	0.74
EL at night												
Production, $/h					3,404	11,277					3,266	10,533
Revenue, $/h					5,860	18,136					5,860	18,136
Profit, $/h					2,456	6,910					2,594	7,603
NightCap, $/h					39.8	79.6					39.8	79.6
P_{rd}, t/h					3.23	3.23					3.23	3.23
C_{prd}, $/t					228	889					228	889
Cp, $/kWh	0.0364	0.1225					0.035	0.115				
Cd, $/kWhe	0.021	0.091					0.03	0.12				
Some decisions												
Pinch	25						5	5				
Dth10	10						4	4				
Efficiency, compressor	0.84						0.87	0.91				
Efficiency, GT	0.9						0.89	0.92				
Efficiency, stream	0.85						0.82	0.87				
Efficiency, pump	0.7						0.92	0.94				

Table 1.3 Sample Combined Cycle/Vapor Compression (CC/VC) System

	Conventional Brine Discharge				Zero Liquid Discharge			
	Reference System		Improved by Lower Production Cost		Reference System		Improved by Lower Production Cost	
Parameter	Oil Price Index, $25/bl	Oil Price Index, $100/bl	Oil Price Index, 25$/bl	Oil Price Index, $100/bl	Oil Price Index, $25/bl	Oil Price Index, $100/bl	Oil Price Index, $25/bl	Oil Price Index, $100/bl
Water, migd	10	10	10	10	10	10	10	10
t/h	1,894	1,894	1,894	1,894	1,894	1,894	1,894	1,894
Power, MW	43.958	43.958	17.455	17.455	77.199	77.199	77.199	77.199
KWh/t	23.21	23.21	9.216	9.216	40.76	40.76	40.76	40.76
Fuel, MW	109.265	109.265	43.9956	39.704	191.895	191.895	190.526	175.563
CO_2, t/h	20.02	20.02	7.895	7.272	35.162	35.162	34.905	32.155
lb/lb fuel	2.7	2.7	2.7	2.7	2.7	2.7	2.7	2.7
lb/kWhe	1.002	1.002	0.995	0.916	1.002	1.002	0.994	0.961
lb/ton water	23.24	23.24	9.17	8.44	40.84	40.84	40.54	37.35
1st-law efficiency	0.4023	0.4023	0.405	0.4396	0.4023	0.4023	0.4052	0.4395
2nd-law efficiency	0.4611	0.4611	0.4617	0.5016	0.4611	0.4611	0.4619	0.5016
Water Side								
Capital, $M	39.4	78.8	104.7	209.5	112.7	225.5	112.7	255.5
Capital, $/h	492.6	985.3	1,309.7	2,619.4	1,410	2820	1,410	2,820
Power side								
Capital, $M	40.06	81.2	14.4	33.2	71.3	142.6	63.7	146.3
$/h	508.0	1,016	1,180.9	415.0	891.7	1,783.5	797.3	1,829
Fuel, $/h	1,092.6	4,370	510.8	1,588.16	1,919	7,675.8	1,905.3	7,022.5
Production C_{wtr}, $/h	2,093.2	6,371.8	1,921.5	4,622.6	4,220.5	12,279	4,112.3	11,671
Production C_{pwr}, $/h	1,600.6	5,386.5	611.8	2,003.1	2,810.6	9,459	2,702.5	8,851.8
C_{wtr} $/t	1.1	3.36	1.01	2.44	3.02	8.8	2.94	8.36

(*Continued*)

Table 1.3 (*Continued*)

	Conventional Brine Discharge				Zero Liquid Discharge			
	Reference System		Improved by Lower Production Cost		Reference System		Improved by Lower Production Cost	
Parameter	Oil Price Index, $25/bl	Oil Price Index, $100/bl	Oil Price Index, 25$/bl	Oil Price Index, $100/bl	Oil Price Index, $25/bl	Oil Price Index, $100/bl	Oil Price Index, $25/bl	Oil Price Index, $100/bl
C_{pwr}, $/kWh	0.0364	0.1225	0.035	0.1147	0.0364	0.1225	0.035	0.1146
Sales								
C_{wtr}, $/t	1.3	2.6	1.3	2.6	1.3	2.6	1.3	2.6
C_{pwr}, $/kWh	0.045	0.20	0.045	0.2	0.45	0.2	0.45	0.2
C_d, $/kWhe	0.021	0.091	0.03	0.12	—	0.091	—	0.12
Leading Decisions								
	VC	CC	VC	CC	VC	CC	VC	CC
	Dtv = 12	Pinch = 25	Dtv = 4.5	Pinch = 5	Psctn = 0.7	Pinch = 25	Psctn = 0.7	Pinch = 5
	Effc = 0.7	Dt10 = 10	Effc = 0.89	Dtcon = 4	Pd = 1.9	Dt10 = 10	Pd = 1.9	Dtcon = 4
	Effp = 0.7	Effc = 0.84	Effp = 0.89	Effc = 0.87	Dtflash = 10	Effc = 0.84	Dtflash = 10	Effc = 0.915
		Effgt = 0.90		Effgt = 0.89	Dtsat = 10	Effgt = 0.90	Dtsat = 10	Effgt = 0.92
		Effstt = 0.85		Effstt = 0.82	Effc = 0.85	Effstt = 0.85	Effc = 0.85	Effstt = 0.87
		Effpmp = 0.7		Effpmp = 0.89		Effpmp = 0.7		Effpmp = 0.93

Notation: Effc, Effgt, Effp, Effsst—compressor, gas turbine, steam turbine efficiencies; Dtv, Dt10, Dtcon, Dtsat: respective temperature differeneces, °F; Pd, Psctn: respective pressures, psia.

Table 1.4 Simple Combined Cycle/Reverse-Osmosis System[a]

	Conventional Brine Discharge				Zero Liquid Discharge			
	Reference System		Improved by Lower Production Cost		Reference System		Improved by Lower Production Cost	
Parameter	Oil Price Index, $20/bl	Oil Price Index, $100/bl	Oil Price Index, 20$/bl	Oil Price Index, $100/bl	Oil Price Index, $20/bl	Oil Price Index, $100/bl	Oil Price Index, $20/bl	Oil Price Index, $100/bl
Water, migd	10	10	10	10	10	10	10	10
Water, t/h	1,894	1,894	1,894	1,894	1,894	1,894	1,894	1,894
Power, MW	12.174	12.174	5.613	5.613	110.46	110.46	110.46	110.46
Power, KWh/t	6.376	6.376	2.919	2.919	58.32	58.32	58.32	58.32
Fuel, MW	30.262	30.262	13.865	12.771	274.57	274.57	272.59	261.191
CO_2, t/h	5.545	5.545	2.54	2.339	50.3	50.3	49.9	46
lb/lb fuel	2.7	2.7	2.7	2.7	2.7	2.7	2.7	2.7
lb/kWhe	1.002	1.002	0.995	0.916	1.002	1.002	0.994	0.916
Ib/ton water	6.44	6.44	2.95	2.72	58.43	58.43	57.96	53.43
1st-law eff	0.4023	0.4023	0.4049	0.4395	0.4023	0.4023	0.4052	0.4397
2nd-law eff	0.4611	0.4611	0.4615	0.5015	0.4611	0.4611	0.4620	0.5018
Water Side								
Capital M$	6.28	13.06	12.834	26.55	0.506	1.012	0.506	1.012
$/h	229	465.1	470.2	951.5	18.98	38.0	18.98	38.0
Power Side								
Capital, $M	11.2	22.5	4.6	10.7	102	204	91.2	209.2
Capital, $/h	140.9	281.7	58.4	134.0	1,275.7	2,551	1,140	2,615.8
Fuel, $/h	302.6	1,210.5	138.6	510.8	2,745.7	10,983	2,726	10,048
$C_{\text{prd wtr}}$, $/h	672.9	1,957.3	667.2	1,596.2	4,040	13,572	3,885	12,701
$C_{\text{prd pwr}}$, $/h	443.3	1,492.2	197	644.8	4,021	13,634	3,866	12,663

(*Continued*)

Table 1.4 (*Continued*)

	Conventional Brine Discharge				Zero Liquid Discharge			
	Reference System		Improved by Lower Production Cost		Reference System		Improved by Lower Production Cost	
Parameter	Oil Price Index, $20/bl	Oil Price Index, $100/bl	Oil Price Index, 20$/bl	Oil Price Index, $100/bl	Oil Price Index, $20/bl	Oil Price Index, $100/bl	Oil Price Index, $20/bl	Oil Price Index, $100/bl
C_{wtr}, $/t	0.355	1.03	0.353	0.84	2.13	7.16	2.05	6.7
C_{pwr}, $/kWh	0.0364	0.1225	0.0351	0.1148	0.0364	0.1225	0.0349	0.1146
Sales								
C_{wtr}, $/t	1.3	2.6	1.3	2.6	1.3	2.6	1.3	2.6
C_{pwr}, $/kWh	0.045	0.2	0.045	0.2	0.045	0.2	0.045	0.2
C_d, $/kWhe	0.021	0.091	0.03	0.12				0.12
Leading Decisions								
	RO	CC	RO	CC	RO	CC	RO	CC
—	$P = 1{,}500$	Pinch = 25	$P = 1{,}000$	Pinch = 5	$P = 1{,}000$, 5,000	Pinch = 25	$P = 1{,}000$, 5,000	Pinch = 5
—	Effp/t = 0.75	Dt10 = 10	Effp/t = 0.88	Dtcon = 4	Effp/t = 0.9	Dt10 = 10	Effp/t = 0.9	Dtcon = 4
—	$A = 0.02$	Effc = 0.84	$A = 0.035$	Effc = 0.916	$A = 0.01$, 0.02	Effc = 0.84	$A = 0.01$, 0.02	Effc = 0.915
—	$B = 0.001$	Effgt = 0.90	$B = 0.0005$	Effgt = 0.92	$B = 0.05$, 0.0003	Effgt = 0.9	$B = 0.05$, 0.0003	Effgt = 0.92
—	$W = 40$	Effstt = 0.85	$W = 40$	Effstt = 0.87	$X_{s1} = 0.04$, 0.041,0.03	Effstt = 0.85	$X_{s1} = 0.04$, 0.041,0.03	Effstt = 0.87
—	$H = 0.05$	Effpm = 0.7	$H = 0.02$	Effpmp = 0.89	$X_{s2} = 0.26$, 0.271, 0.0005	Effpmp = 0.7	$X_{s2} = 0.26$, 0.271, 0.0005	Effpmp = 0.94

[a] See notations footnote in Table 1.3 and Nomenclature Section (at end of chapter) for abbreviation and symbol definitions.

Table 1.5 Reverse-Osmosis/Photovoltaic Systems

	Runs								
Parameter	1	2	3	4	5	6	7	8	9
Input									
A_{wtr}, lb/(h · ft^2· psi)	0.04	0.04	0.04	0.04	0.04	0.04	0.01	0.002	0.01
B_{salt}, ft/h	0.0005	0.0005	0.0005	0.0005	0.0005	0.0005	0.0005	0.0003	0.0008
Top pressure, psia	900	900	900	900	900	900	1,250	1,800	600
H_{brn} flow, in.	0.06	0.06	0.06	0.01	0.06	0.01	0.05	0.015	0.015
PV cell type	1	2	3	1	1	3	1	1	1
Cell lab efficiency	0.13	0.14	0.19	0.13	0.09	0.19	0.13	0.13	0.13
$/peak, W	0.308	6.15	4.34	2.50	5.67	3.53	3.08	3.08	3.08
Solar flux, kW/m^2	0.65	0.65	0.65	0.8	0.5	0.8	0.65	0.65	0.65
Operation days per year	365	365	365	365	240	365	365	365	365
Eff pump/turbine, each	0.9	0.9	0.9	0.9	0.8	0.9	0.9	0.9	0.9
X_{salt} feed, lb/lbm	0.04	0.04	0.04	0.04	0.04	0.04	0.04	0.04	0.01
$X_{salt\ reject}$, lb/lbm	0.07	0.07	0.07	0.07	0.07	0.07	0.07	0.07	0.04
Field	0.85	0.85	0.85	0.85	0.60	0.85	0.85	0.85	0.85
Output									
Product salt, ppm	467	467	487	201	467	201	484	489	494
RO surface, ft^2	14,809	14,809	14,809	9,491	14,826	9,491	17,892	45,857	35,209
PV surface, ft^2	17,109	15,096	11,665	15,885	42,412	10,830	23,767	37,820	10,177
Power, kW	129	120	129	148	174	148	179	286	77
EO dissipation, kW	102	102	102	120	147	120	152	258	49
PV dissipation, kW	902	780	573	1,030	1,793	655	1,253	1,993	536
RO process efficiency	0.32	0.32	0.32	0.28	0.24	0.28	0.23	0.15	0.19
RO mmbr number	1,593	1,593	1,593	4,780	1,591	4,780	1,549	1,732	1,255
Pressure, φ_p	1.2	1.2	1.2	1.6	1.2	1.6	1.8	3.6	2.0
ΔP_{brn}, psi	3.1	3.1	3.1	402	3.1	402	6.5	606	197
Average H_{mass}, ft/h	0.197	0.197	0.197	0.776	0.197	0.776	0.210	0.345	0.293
$25/bl economy (0.05,0.5)									
Capital, $M	0.612	1.017	0.779	0.509	1.212	0.664	0.813	1.536	0.732
PV unit cost $/ft^2	23.7	53.7	49.1	23.7	23.7	49.1	23.7	23.7	23.7
C_{pwr} $/kWh (0.05)	0.107	0.215	0.152	0.087	0.723	0.123	0.107	0.107	0.107
C_{wtr} $/m^3 (0.5)	0.673	0.940	0.783	0.508	1.624	0.610	0.862	1.849	1.126
Competitiveness	Near	—	Near	Yes	—	Near	Near	—	—
$100/bl economy (0.2,1)	—	—	—	—	—	—	—	—	—
Capital, $M	1.224	2.035	1.558	1.018	2.424	1.328	1.625	3.071	1.462
PV unit cost, $/ft^2	47.4	107.4	98.1	47.4	47.4	98.1	47.4	47.4	47.4
C_{pwr}, $/kWh (0.2)	0.215	0.430	0.303	0.175	0.602	0.247	0.215	0.215	2.15
Water cost, $/m^3 (1)	1.347	1.879	1.566	1.016	3.248	1.220	1.723	3.698	2.252
Competitiveness	Almost	—	Near	Yes	—	Almost	Near	—	—

Table 1.6 Photovoltaic/Electrodialysis Systems

	Runs								
Parameter	1	2	3	4	5	6	7	8	9
Inputs									
Feed, ppm	5,000	5,000	5,000	5,000	5,000	5,000	2,000	10,000	10,000
Product, ppm	500	500	500	500	500	500	500	300	500
ED desalting efficiency	0.3	0.3	0.3	0.6	0.1	0.5	0.3	0.3	0.6
Applied voltage	120	120	120	120	60	120	60	120	60
Current densityAmp/m^2	100	100	100	100	50	100	50	100	50
Brine recycle ratio	0.8	0.8	0.8	0.0	0.85	0.8	0.0	0.8	0.0
PV cell type	11	22	33	11	11	33	11	11	11
Cell lab efficiency	0.1275	0.145	0.187	0.135	0.09	0.187	0.1275	0.1275	0.135
$/peak W	3.077	6.154	4.344	2.361	5.667	3.529	3.077	3.077	2.906
Solar flux, kW/m^2	0.65	0.65	0.65	0.8	0.5	0.8	0.65	0.65	0.65
Operation days per year	365	365	365	365	240	365	365	365	365
Field desalination-efficiency	0.85	0.85	0.85	0.9	0.60	0.85	0.85	0.85	0.9
Output									
W_{theor}, Btu/lb produced	0.19	0.19	0.19	0.12	0.21	0.19	0.18	0.25	0.17
ED surface, m^2	55.4	55.4	55.4	17.9	725.6	33.2	207.8	71.6	96.7
PV surface, m^2	2,406.6	2,123.4	1,640.8	602.4	14,473.2	801.9	2,257.3	3,106.4	996.2
Power, kW	195.53	195.53	195.53	63.79	638.52	117.61	183.41	252.39	85.70
ED dissipation, kW	202	202	202	29	652	124	150	270	38
PV dissipation, kW	1,365	1,181	867	417	6,585	522	1,289	1,762	560
ED overall efficiency	0.299	0.299	0.299	0.593	0.100	0.497	0.299	0.299	0.595
ED membrane number	55	55	55	18	726	33	208	72	97
ΔP flow, psi	0.3	0.3	0.3	0.3	0.3	0.3	0.3	0.3	0.3
Reject brine X_{salt} ppm	27,511	27,511	27,511	9,502	35,015	27,511	3,501	58,515	1,905
Brine X_{salt}, ppm	23,009	23,009	23,009	5,000	30,513	23,009	2,000	48,812	10,000
$25/bl economy (0.05,0.5)	—	—	—	—	—	—	—	—	—
Captl $M	0.62	1.23	0.87	0.16	3.78	0.43	0.60	0.80	0.27
PV unit cost $/$m^2$	255	578	528	255	255	528	255	255	255
C_{pwr}, $/kWh (0.05)	0.107	0.215	0.152	0.082	0.301	0.123	0.107	0.107	0.102
C_{wtr}, $/$m^3$ (0.5)	0.044	0.089	0.063	0.011	0.406	0.031	0.042	0.057	0.018
Competitiveness	Near	—	—	Yes	—	Near	Near	Almost	Almost
$100/bl economy (0.2,1)	—	—	—	—	—	—	—	—	—
Capital, $M	1.24	2.47	1.75	0.31	7.56	0.85	1.20	1.60	0.53
PV unit cost, $/$m^2$	510	1,156	1,056	510	510	1,056	510	510	510
C_{pwr}, $/kWh (0.2)	0.215	0.430	0.303	0.165	0.602	0.247	0.215	0.215	2.03
Water cost $/$m^3$ (1)	0.089	0.177	0.125	0.022	0.811	0.061	0.083	0.114	0.037
Competiteness	Near	—	—	Yes	—	Near	Near	Yes	Yes

Table 1.7 Osmosis Power

Parameter	Runs								
	1	2	3	4	5	6	7	8	9
Input									
A_{wtr} lb/(h · ft^2 · psi)	0.04	0.04	0.03	0.03	0.02	0.02	0.01	0.01	0.05
B_{salt}, ft/h	0.0005	0.0	0.0006	0.0	0.0005	0.0	0.001	0.0	0.0003
X_{salt} high, lb/lbm	0.1	0.1	0.07	0.07	0.15	0.15	0.2	0.2	0.25
X_{salt} reject, lb/lbm	0.06	0.06	0.05	0.05	0.06	0.06	0.06	0.08	0.06
$H_{c_{high}}$, in.	0.6	0.6	0.4	0.4	0.2	0.2	0.5	0.5	0.6
$H_{c_{low}}$, in.	0.5	0.5	0.5	0.5	0.3	0.3	0.4	0.4	0.5
Output									
X_{leak}, ppm	421	0	673	0	841	0	3356	0	202
A_{wall}, M · ft^2	41.2	45.6	110.8	118.4	75.6	55.0	81.8	66.0	13.8
A_{bulk}M · ft^2	39.6	39.6	107.4	107.4	50.0	50.0	78.6	61.3	13.2
Net power, MW	2.5	2.5	0.5	0.4	7.5	7.4	13.1	15.1	17.2
Ideal power, MW	34.3	34.3	6.2	6.2	68	68	80.1	72.9	749.2
∂X_{plzn}, high, lb/lbm	1.2	1.2	0.042	0.042	0.405	0.405	0.842	0.720	1.425
∂X_{plzn}, low, lb/lbm	0.042	0.180	0.012	0.068	1.178	0.093	0.024	0.096	0.023
$25/bl economy									
Capital wall, $M	494.1	546.9	1,329.1	1,420.2	907.4	650.8	981.7	793.2	166.1
Capital bulk, $M	475.4	475.6	1,288.4	1,289.3	604.9	605.4	937.7	735.1	158.2
Capital wall, $/kWh	4.45	5.55	24.29	27.88	2.42	2.56	2.01	2.33	0.22
Capital bulk, $/kWh	4.09	4.09	22.75	22.75	2.07	2.07	1.75	1.95	0.19
Capital ideal, $/kWh	3.44	3.44	19.11	19.11	1.73	1.73	1.47	1.62	0.161
$100/bl economy									
Capital wall, $M	988.1	1,093.8	2,658.3	2,840.4	1,814.8	1319.6	1963.3	1,584.4	332.3
Capital bulk, $M	950.8	951.8	2,576.8	2,578.6	1,209.8	1210.8	1875.3	1,470.1	316.5
Capital wall, $/kWh	8.9	11.09	48.57	55.76	4.87	5.12	4.01	4.67	0.44
Capital bulk, $/kWh	8.18	8.18	45.50	45.50	4.13	4.13	3.51	3.85	0.37
Capital ideal, $/kWh	6.87	6.87	38.22	38.22	3.74	3.74	2.95	3.24	0.31

The results have been presented in tabular rather than graphical format because of the large number of decision variables. Thermodynamic decision variables are no less than 15 for any system, and the thermodynamic decisions trigger both design and manufacture decisions because of the design and manufacture degrees of freedom involved. Graphs are more transparent in presenting results for cases of one or two decision variables. The number of two and three-dimensional relations explodes, however, with a large number of decision variables.

1.4 THE ANALYZED SYSTEMS IN DETAIL

1.4.1 Gas Turbine/Multistage Flash Distillation Cogeneration Systems

1.4.1.1 Flow Diagram Figure 1.1 is a flow diagram showing a steam turbine both idle and refiring active under less than design power load. Ejector steam and blowdown are allowed for. Airblade cooling for higher firing temperature is allowed for but not employed. The system has 63 thermodynamic decision variables, 24 of which can be manipulated to improve its cost objective function of higher profitability.

1.4.1.2 Major Features of the Results

- A night product raises the load factor from 0.583 to 0.865 and produces 5625 t/h desalted water <500 ppm, assuming an RO power requirement of 5 kWh/t. Profitability is reduced in the absence of a night product and is raised to 5–10 times the design steady-state value in the presence of a night product, provided all night product is salable.
- The CO_2 emission is slightly reduced from 64 to 56 t/h with higher profitability since burning fuel by refiring is essential to maintain the steady production of the MSF distiller. Auxiliary boilers and the throttling of high-pressure steam are alternatives that maintain the steady production of MSF distiller with the same weak effect on CO_2 emission.
- The cost of water remains around \$1/t and the cost of power around \$0.038/kWh for \$25/bl economy. For \$100/bl economy the costs are $\sim$ \$3/t for water and $\sim$ \$0.12/kWh for power.
- The first- and second-law efficiencies are raised from their design values of 0.3 and 0.355 to 0.37 and 0.405, respectively, with higher profitability.
- Automated optimization changes all the 24 manipulated decision variables. For example, the number of MSF stages is raised for its design value of 18 to 28, the pinch point is reduced from 50°F to around 10°F, and the level of adiabatic efficiencies of compressor, gas turbine, and steam turbine is raised from 0.85 to 0.92 for higher profitability.
- The improved design points differ for each of the two economies considered, namely, \$20/bl and \$100/bl oil.

- The fuel penalty of actual control compared to ideal control (the design efficiency remains constant at all load fractions) for the reference system is 26 MW with no night product. This corresponds to \$260/h for \$20/barrel economy and to \$1042/h for \$100/bl economy. The penalty for higher profitability is only about 7 MW with a night product of desalted water. This corresponds to \$70/h for a \$25/bl economy and to \$280/h for \$100/bl economy

1.4.2 The Simple Combined Cycle Systems

1.4.2.1 Flow Diagram Air-cooling (see Fig. 1.2) of blades is allowed for but not employed since the firing temperature is only up to 1600°F. The steam turbine expands steam to condensing temperature of 100°F. The power to be delivered after system needs have been satisfied is set to 100 MW. The number of thermodynamic decision variables is 34, 18 of which manipulated to lower production cost.

1.4.2.2 Major Features of the Results

- A night product raises the load factor from 0.583 to 0.865 and produces 5625 t/h desalted water <500 ppm during installation of a night RO desalter of currently attainable power requirement of 5 kWh/t and produces 0.36 t/h H_2 and 2.88 t/h O_2 during installation of a night water electrolyzer of power requirement 78.25 MWh/t H_2, which represents ΔG_f of the water content divided by an efficiency factor of 0.42 for a direct-current intensity of 1 A/cm^2. Profitability becomes a loss in the absence of night products and is raised to 5–10 times the design steady-state value in the presence of night products, provided all night products are salable.
- The CO_2 emission design value is 45 t/h (compared to 64 t/h of the GT/MSF case). The emission is reduced to 40 and 36 t/h with improved lower production cost.
- The cost of power is ~ \$0.035/kWh for 25\$/barral economy and ~ \$0.12/kWh in \$100/bl economy.
- The first- and second-law efficiencies are raised from their design values of 0.4 and 0.46 to 0.43 and 0.465, respectively, for lower production cost.
- The fuel penalty of actual control compared to ideal control is 19.5 MW with no night product. This corresponds to \$195/h for \$25/bl economy and to \$781/h for a \$100/bl economy. The penalty for lower production cost is only ~5.5 MW, with a night product of desalted water or of H_2 and O_2. This corresponds to \$59/h for a \$25/bl economy and to \$220/h for \$100/bl economy.
- The cost of night product of water is a \$0.24/t, and that of H_2 and O_2 is \$228/t for a \$25/bl economy. For a \$100/bl economy, the corresponding costs are \$0.74/t and \$889/t.

1.4.3 Vapor Compression Systems Driven by the Figure 1.2 Simple Combined Cycle

1.4.3.1 Flow Diagrams Figure 1.3 shows a vapor compression (VC) distiller with 16 thermodynamic decision variables, three of which are manipulated to lower production cost. The operating temperature is maintained at 160°F.

Figure 1.4 shows its version of Figure 1.3 for zero liquid discharge (ZLD) with 19 decision variables, none of which are manipulated for lower production cost. Compressor efficiency is set at 85%, with a of pressure ratio of 2.73 and a suction pressure of 0.7 psia. This low suction pressure calls for more than 10 compressors of reasonable inlet area operating in parallel.

Both VC versions are driven by the simple combined cycle shown in Figure 1.2, with 34 decision variables, 18 of which are manipulated to lower production cost.

1.4.3.2 Major Features of the Results

- No night product is introduced because the production is at steady state, producing 10 migd water by VC desalter.
- The reference design of the VC distiller has a capital cost of $39M for compressor and heat exchange surfaces and requires 44 MW power. The driving simple combined cycle (SCC) requires, in turn, 109 MW fuel. For a $25/bl economy, the cost of water is $1.1/t. The cost of power is as delivered by the combined cycle $0.0364/kWh. For a $100/bl economy, the cost of water is $3.36/t and the cost of power as delivered by the combined cycle is $0.1225/kWh.
- The improved design by lower production cost has a capital cost of $210M and requires 17.5 MW power. The driving SCC requires, in turn, 40 MW fuel. For a $25/bl economy, the cost of water is $1.1/t and the cost of power as delivered by the combined cycle is $0.035/kWh. For a $100/bl economy, the cost of water is $2.44/t and the cost of power as delivered by the combined cycle is $0.115/kWh.
- The concept of zero liquid discharge is considered using single-stage VC. The result, so far, has not been cost-effective. Power requirement is almost doubled (77 MW), and so is CO_2 emission (35 t/h). The unit cost of water almost tripled. However, the high pressure of the RO case is avoided but large parallel compressors operating under vacuum are needed. Section 1.A.4 explains the large power requirement via the theoretical work of separation extended to zero liquid discharge.

1.4.4 Reverse Osmosis Desalination Systems Driven by the Figure 1.2 Simple Combined Cycle

1.4.4.1 Flow Diagrams Figure 1.5 shows conventional single- (a) and two-stage (b) reverse-osmosis desalination systems. The two-stage system is only a standby system in case product water at concentrations of <500 ppm cannot be

obtained by the single-stage system. The standby option, however, was not required. The single-stage system has 18 thermodynamic decision variables, 12 of which are manipulated to minimize production cost with product quality <500 ppm.

The design model of the RO process [15], which is based on numerous equations [the model is shown in the following diagram, and the equations include Eqs. (1.22)–(1.31)], and does not have many design degrees of freedom; moreover, solutions with quality for product water >500 ppm have to be excluded:

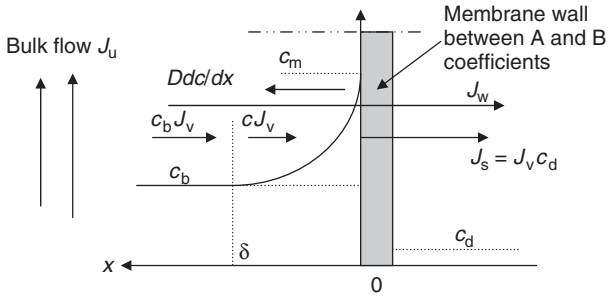

$$J_w = A(\Delta P - \Delta\Pi) = A[(P_m - P_d) - (\Pi_m - \Pi_d)]$$
$$= A[(P_m - P_d) - \varphi RT(c_m - c_d)] \tag{1.22a}$$

$$J_s = B(\Delta c) = B(c_m - c_d) \tag{1.23a}$$

$$J_v = h_m \left[\ln\left(\frac{c_m - c_d}{c_b - c_d}\right)\right] \tag{1.24a}$$

where

$$J_v(c - c_d) - Ddc/dx = 0 \tag{1.25}$$

$$\int_{x=0}^{\delta} J_v dx = \int_{c_m}^{c_b} D\,\mathrm{dc}/(c - c_d) \tag{1.26a}$$

$$J_v\delta/D = \frac{J_v}{h_m} = \ln\left[\left(\frac{c_m - c_d}{c_b - c_d}\right)\right] \tag{1.26b}$$

$$\delta = D/h_m \tag{1.27}$$

$$J_w = J_v(\rho - c_d) \tag{1.28}$$

$$J_s = J_v c_d \tag{1.29}$$

$$S_{RO} = \frac{M_d}{J_w + J_s} \tag{1.30}$$

$$Z_{RO} = C_{aRO} S_{RO} \tag{1.31}$$

where C_{aRO} is the membrane cost per unit membrane surface area. A multiplier >1 accommodates care of the balance of plants (default 1.5).

Equations (1.22a)–(1.24a), (1.28), and (1.29) are five equations in five unknowns J_w, J_s, J_v, c_m and c_d. The number of equations and unknowns can be reduced to 3 by substituting Equations (1.28) and (1.29) in Equations (1.22a)–(1.24a), and the equations and the unknowns may be reduced to 3:

$$J_w = A[(P_m - P_d) - \varphi RT(c_m - c_d)] \tag{1.22b}$$

$$= B(c_m - c_d)\frac{(\rho - c_d)}{c_d} \tag{1.23b}$$

$$= h_m(\rho - c_d)\left[\ln\left(\frac{c_m - c_d)}{c_b - c_d}\right)\right] \tag{1.24b}$$

The unknowns are J_w, c_m, and c_d.

The following equations are needed to compute pressure losses and mass transfer coefficient h_m and hence concentration boundary-layer thickness d. The equations are based on dimensional analysis. Note that the assumption of single-thickness boundary layer is often used in the analysis of RO membranes. Baker [16, p. 176] uses $\delta = 20$ μm. This assumption is relaxed by dimensional-analysis-based equations, where the thickness responds to geometry changes of flow conduit.

$$f = 16/N_{RE} \quad \text{for fully developed laminar flow} \tag{1.32}$$

$$= 0.078{N_{RE}}^{-0.25} \quad \text{for fully developed turbulent flow}, N_{RE} < 30,000 \tag{1.33}$$

$$N_{SH} = 1.85\left(\frac{N_{PE}}{N_V}\right)^{1/3} \text{ to asymptotic value of } N_{SH}N_{PE} = 48 \tag{1.34}$$

for laminar flow between plates(narrow passages)

$$= 1.62\left(\frac{N_{PE}}{N_V}\right)^{1/3} \text{ to asymptotic value of } N_{SH}N_{PE} = 16 \tag{1.35}$$

for laminar in tubes, $N_{Re} < 1000$

$$= 0.04N_{RE}^{0.75}{N_{SC}}^{0.33} \tag{1.36}$$

for fully developed turbulent flow, $N_{RE} > 10,000$

$$N_{RE} = \text{Reynolds number} \quad = Ud\frac{\mu}{\rho} \tag{1.37}$$

$$N_{PE} = \text{Peclet number} \quad = V\frac{d}{D} \tag{1.38}$$

$$N_{SH} = \text{Sherwood number} \quad = h_m \frac{d}{D} \tag{1.39}$$

$$N_{SC} = \text{Schmidt number} \quad = \mu / \frac{\rho}{D} \tag{1.40}$$

$$N_v = \text{permeated/flow velocity geometry} = J_v \frac{l}{J_u / d} \tag{1.41}$$

J_v = velocity normal to flow(x direction)

J_u = velocity in flow direction

l = length in brine flow direction

d = equivalent diameter of the brine flow area (hydraulic diameter)

$$d = 4WHn_1/2/(W + H)/n_2 \tag{1.42}$$

n_1 = blockage factor of brine flow area

n_2 = wetted perimeter increase factor

The factors n_1 and n_2 depend on the thickness and the shape of feed spacers. The factors produce an equivalent reduced height H_e of an empty conduit. The values assigned to n_1 and n_2 in this model are 0.25 and 2.0, respectively. An empty conduit has $n_1 = n_2 = 1$.

The diffusion coefficient computed by Wilke–Chang equation [17, Reid p. 598] $= 3.55 \cdot 10^{-6}$ cm^2/s. The diffusion coefficient quoted from Baker [16, p. 176] $= 10 \cdot 10^{-6}$ cm^2/s, is used in this model. Density ρ and viscosity μ are computed by transport properties routine of reference [14].

A membrane relation that guarantees an allowable product salt content (e.g. <500 ppm) may be derived by introducing a membrane dimensionless number N_m as follows. First, the wall osmosis pressure difference $(\Pi_m - \Pi_d)$ may be written in terms of wall and product salt concentrations (mass or mole per unit volume):

$$(\Pi_m - \Pi_d) = \varphi RT(c_m - c_d) \tag{1.43}$$

where $\varphi = 1$ for ideal solution and > 1 to accommodate deviations from ideal solution. In this study, ideal solution is assumed.

Applied pressure $(P_m - P_d)$ may be written in a similar way by introducing φ_P:

$$(P_m - P_d) = \varphi_P RT(c_m - c_d) \tag{1.44}$$

$$\frac{J_w}{J_s} = A(\varphi_P - \varphi)R\frac{T}{B} = N_M \tag{1.45}$$

Equation (1.45) is realized in this model development and is believed to be important in RO membrane design. It presents the combined influence of membrane

coefficients and applied pressure (A, B, and P). The invested pressure above osmosis is measured by $\varphi_P - \varphi$, where $\varphi = 1$ for ideal solutions.

The following are some features of N_M:

- For seawater, $N_M > 1500$ seems to guarantee product <500 ppm.
- The larger the N_M, the lower the membrane surface requirement for a given product rate.
- N_M is independent of concentration polarization.

A unit of 200 usgpd is considered (surface $\sim$1 m^2). Its flow path is divided into five sections. The feed concentration is equal to the bulk concentration to first section. All the parameters of interest along the flow path of each section are computed. For each section, the permeated flux J_w and membrane concentrations c_m and c_d are obtained by solving Equations (1.22b)–(1.24b) simultaneously. The unit modules and their pressure shells can be arranged in numerous ways to manage flow pressure losses and shell diameter. A module of 30 units in parallel is selected. A shell contains three modules in series. About 18 shells provide the required product rate of 415 m^3/d (0.11 usmgd). This satisfies the domestic water demands of a community of about 1000 persons (0.3 m^3 per day per person).

Figure 1.6 depicts a version of a RO with zero liquid discharge of two stages. The number of stages depends on the solubility limits of the various salt species. In the absence of membranes selective to specific salt species, Figure 1.6 assumes a hypothetical version of two stages: (1) a retainer for species other than sodium chloride and (2) a retainer to sodium chloride. The system has 27 decision variables, 12 of which are manipulated for production cost minimization.

1.4.4.2 Major Features of the Results

Please refer to Table 1.4 for sample runs

- No night product is introduced because the production is at steady state, producing 10 migd water by an RO desalter
- The reference design of the RO desalter has a membrane surface of 402,452 ft^2 and requires 12.17 MW power (6.376 kWh/t water product). The driving simple combined cycle (SCC) requires, in turn, 30.3 MW fuel. For a $25/bl economy, the cost of water is $0.35/t. The cost of power is as delivered by the combined cycle $0.0364/kWh. For a $100/barrel economy, the cost of water is $1.03/t and the cost of power as delivered by the combined cycle is $0.1225/kWh.
- The improved design by lower production cost has a membrane surface of 806,080 ft^2 and requires 5.6 MW power (2.919 kWh/t water product). The driving simple combined cycle requires, in turn, 13.86 MW fuel. For a $25/barrel economy, the cost of water is $0.35/t and the cost of power as delivered by the combined cycle is $0.035/kWh. For a $100/bl economy, the cost of water is $0.84/t and the cost of power as delivered by the combined cycle is $0.1148/kWh.

- For RO, the reference system main decision variables are water coefficient 0.02 lb/(h.ft^2·psi), salt coefficient 0.015 ft/h, and pressure 1500 psia. For CC, the main decisions are pinch 25°F, compressor efficiency 0.85, and turbine efficiency 0.9.
- The concept of zero liquid discharge is considered using two stages in series. The result, so far, has not been cost-effective. The power requirement increased about 8 times, and CO_2 emission almost doubled. Moreover, high-pressure membranes (5000 psia), probably ceramic, need to be developed. The large power requirement via the theoretical work of separation extended to zero liquid discharge is discussed in Section 1.A.4.

1.4.5 Photovoltaic/Reverse-Osmosis (PV/RO) Solar Systems

1.4.5.1 Flow Diagram Figure 1.7 shows the flow diagram of the solar desalter of small distributed 0.2 migd desalted water for communities of about 10,000 people along with the main variables of the RO subsystem and of the solar subsystem. Figure 1.8 shows the future potential of this particular solar desalting system. Figure 1.9 shows two photovoltaic/electrodialysis (PV/ED) configurations.

1.4.5.2 Major Features of Results Please refer to Table 1.5 for sample runs

- All runs use inputs of attainable membrane water and salt coefficients
- The first eight runs assume seawater feed of 0.04 salt mass-fraction and reject around 0.07 salt mass fraction. The last assume brackish-water feed of 0.01 salt mass fraction and reject 0.04 mass fraction.
- Solar intensity ranged from 0.5 to 0.8 kW/m^2, averaging 0.65 kW/m^2.
- All runs assume operation of 365 days per year except run 5, which assumes 240 days per year.
- All runs assume loss of cell field efficiency to 0.85 of that laboratory evaluation.
- For a $25/bl oil price index economic environment, a competitive power cost of $0.05/kWh and a competitive water cost using RO of 0.5 $/m^3 can be assumed. One run is competitive. A few runs are nearly competitive, utilizing the advantage of no CO_2 emission.
- For $100/bl oil price index economic environment, the competitive power cost is $0.2/kWh (4 times that of the $25/bl index) and a competitive water cost using RO of $0.1/m^3 (2 times that of the $25/bl index) can be assumed. Competitiveness increases because the cost of a material product escalates at a lower rate than does power cost.
- Figure 1.8 indicates a promising potential future for PV/RO desalination technology [18].

1.4.6 Photovoltaic/Electrodialysis Solar System

The separated PV/ED is the configuration (Fig. 1.9b) considered for analysis. The feed is assumed to have zero exergy. A simple analysis model is assumed that does not reveal the distributions of salt and water through flow passages because of insufficient information on ion exchange membranes.

1.4.6.1 Major Features of the Results Please refer to Table 1.6 for sample runs

- Efficiencies are used as decisions rather than being computed whenever the available characteristics of the active surface (membrane or solar cell) do not permit computiation of the efficiency.
- All runs use inputs of attainable or near attainable efficiencies. Ion exchange membrane efficiencies ranged from 0.1 to 0.6. Pump efficiency was set at 0.8. DC–AC conversion efficiency was set at 0.95.
- The first six runs assume feed of 5000 ppm salt content. One run assumes feed of 2000 ppm and one run assumes feed of 10,000 ppm.
- The brine recycle ratio is 0.8 for most runs. For one run the ratio is 0.85. For three runs the ratio was set to zero.
- Solar intensity ranged from 0.5 to 0.8 kW/m^2 and averaged 0.65 kW/m^2.
- All runs assume operation of 365 days per year except run 5, which assumes 240 days per year.
- The first three runs compare the three types of solar cells, each at its upper efficiency.
- Eight runs assume loss of cell field efficiency to 0.85 of that laboratory standard test values. One run limits the loss to 0.9 the standard test value.
- For \$25/bl oil price index economic environment, a competitive power cost of \$0.05/kWh and a competitive water cost using RO \$0.5/m^3 can be assumed. One run is competitive. A few runs are nearly competitive, utilizing the advantage of no CO_2 emission.
- For \$100/bl oil price index economic environment, the competitive power cost is \$0.2/kWh (4 times that of the \$25/bl index) and a competitive water cost using ED of \$0.1/m^3 (2 times that of the \$25/bl index) can be assumed. Three runs show competitiveness. Competitiveness increases because the cost of a material product escalates at a lower rate than power cost.

1.4.7 Osmosis Power Systems

1.4.7.1 Flow Diagram Figure 1.10 shows the flow diagram of a single-stage osmosis power system utilizing the chemical exergy difference between two streams of brines of different salt concentration. The less concentrated brine is assumed to be seawater of salt mass fraction 0.04. Water mobility through water-selective

membranes is assumed. The stage is divided into 10 cells. The major controlling variables of a cell are given in Figure 1.10b.

However, the issue of tapping power from the chemical exergy difference between two brine streams of different salt concentrations by an electrodialysis device using the mobility of salt ions through ion exchange selective membranes,

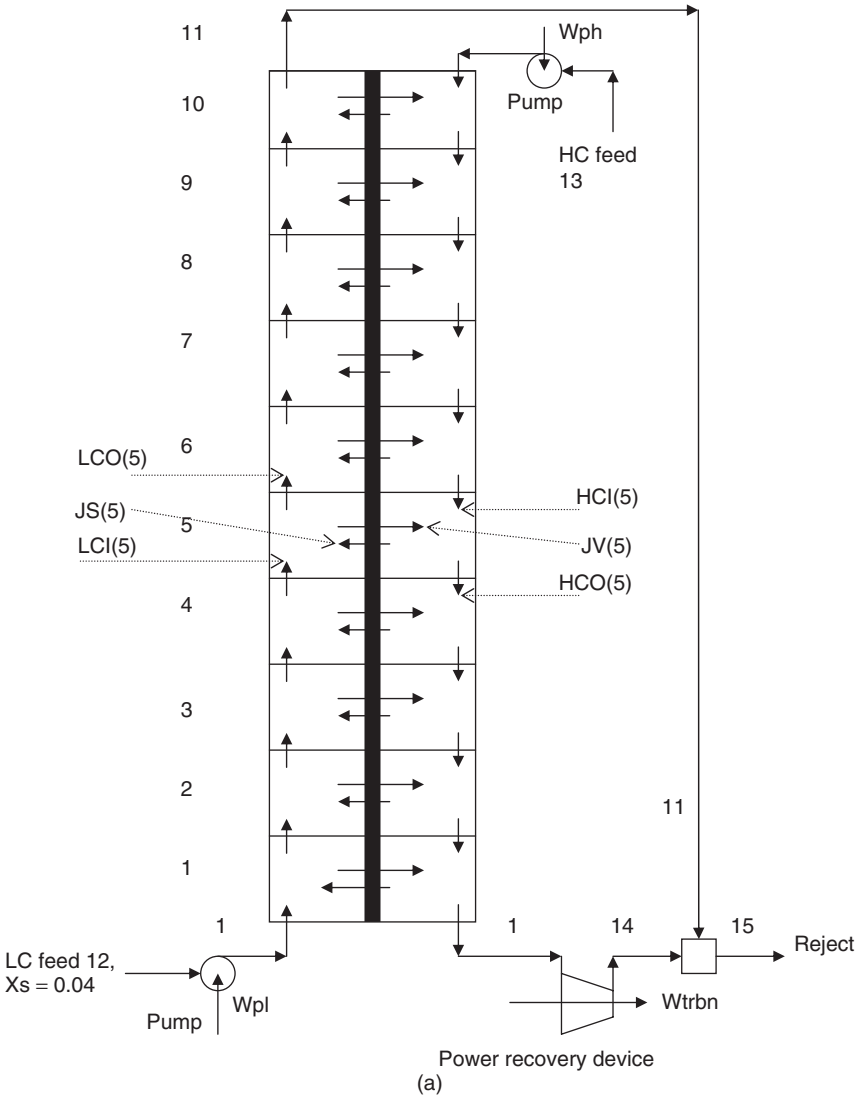

Figure 1.10 The osmosis power system: (a) flow diagram; (b) variables controlling the cell [19].

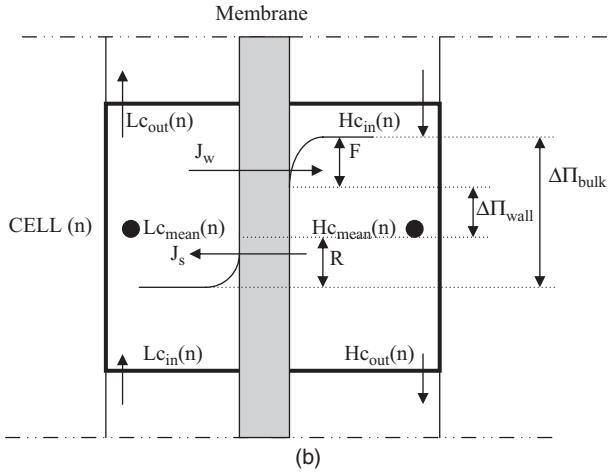

Figure 1.10 (*Continued*)

remains to be addressed. Consider the following equations:

$$\Delta\Pi_{\text{bulk}} = \varphi RT\left(\rho_{c_{\text{high bulk}}} XS_{c_{\text{high bulk}}} - \rho_{c_{\text{low bulk}}} XS_{c_{\text{low bulk}}}\right) \tag{1.46}$$

$$\Delta\Pi_{\text{wall}} = \Delta\Pi_{\text{bulk}} - F - R \tag{1.47}$$

where F is the fall in the salt content of the high-concentration fluid due to dilution by the diffusing pure water flux J_w to the high-concentration side of the membrane causing a polarization effect $\partial X_{\text{plzn high}}$ and R is the rise in the salt content of the low concentration fluid due to loss of diffusing pure water flux J_w to the high concentration side of the membrane and the diffusing salt flux J_s to the low concentration side, causing a polarization effect $\partial X_{\text{plzn low}}$. Also, $J_s = 0$ for membrane salt permeability coefficient $B \approx 0$:

$$\text{Work recovered} = A(\Delta\Pi_{\text{wall}} - \Delta P)\Delta P \tag{1.48}$$

$$\text{Theoretical work recovery } W_{\text{theor}} = \frac{A}{4}\Delta\Pi^2{}_{\text{bulk}} \tag{1.49}$$

1.4.7.2 Major Features of the Results Please refer to Table 1.7 for sample runs

- Table 1.7 shows a sample result of inputs and outputs of the osmosis power systems of a concentrated feed stream of 10 migd of salt mass fractions 0.07–0.25 relative to seawater with a salt mass fraction of 0.04 for the economies of $25 and $100 per barrel of oil.

- Power from conventional salt content of rejected brine (0.06–0.08 lb_{salt}/lb_{mix}) due to concentration difference is not cost-effective. A small amount of power < 0.5 MW is gained by large membrane surface $110M \cdot ft^2$. For brine with a salt mass fraction of 0.25, a power as high as 20 MW is gained by a membrane surface around 12 M ft^2. Only for a brine of salt content 0.1 and higher does power recovery begin to make sense.
- For a \$25/bl (oil price index) economy and brine of salt mass fraction <0.1, power cost is as high as \$25/kWh. The power cost for a corresponding ideal process is \$19/kWh. For brine of salt mass fraction 0.25, power cost is reduced to \$0.2–0.4/kWh. The power cost for a corresponding ideal process is \$0.16/kWh. For the \$100/bl, economy, the respective costs are doubled.
- The salt mass fraction of brine from oilwells can be as high as 0.25. Power generation by this brine, when combined with seawater via membranes, can be cost-effective in some situations.

1.4.8 Future Competitiveness of Combined Desalination Systems

1.4.8.1 Prediction Criteria Efficiency, dumped waste and product cost are three major criteria that identify the most fit desalination system in the future. Overall system efficiency, CO_2 emission per unit product, and cost/unit product are considered for the systems analyzed. Dumped brine is assumed to be tolerated because zero liquid discharge is still far from being cost-effective.

1.4.8.2 Predicted Competitiveness GT/MSF systems show that the case of variable power demand cogeneration counteracts most of the advantage of cogeneration. This widely used cogeneration is likely to loose attractiveness in the future. The advantage is, however, maintained for base power load cogeneration.

SCC systems for power generation show that power-driven night products of low storage cost improves the plant load factor and raises its profitability provided the products are in short supply. The management of power generation by organized night products may gain competitive advantage in the future.

The CC/RO desalting systems show that the attractiveness of power driven desalting systems is likely to surpass that of distillation because of higher efficiency, lower emissions and lower product cost. The CC/VC desalting systems come second to CC/RO. The lower operation pressure and the higher biofouling resistance are advantages, but the handling of large specific volumes is a disadvantage. The development of strong light material for high-speed low-pressure-ratio compressors, or the development of scale-free VC operation at atmospheric pressure, reduce the disadvantage as well as the gap between the product cost by RO and VC. If the disadvantage is reduced, the power-driven VC will gain also achieve future promise for zero-liquid-discharge (ZLD) desalination.

The PV/RO system has zero CO_2 emission and zero fossil fuel consumption but does not avoid dumping of concentrated brine in the physical environment. Their future attractiveness is on the rise. The PV/ED system comes second to PV/RO if it undergoes sufficient development.

The osmosis system for power production is only a possibility, not a reality, and requires the availability of brine near saturation to combine with seawater to obtain power at acceptable cost. If developed, it can be useful for eliminating product water of oilfields located near a sea.

References listed in Section 1.F.9 at the end of this chapter are additional useful readings for the preceding Section 1.4.

1.5 RECOMMENDED RESEARCH DIRECTIONS

1.5.1 Avoiding CO_2 Emissions

- Desalination systems driven by renewable energy sources, particularly solar, are recommended if CO_2 emission is to be avoided.
- Competitiveness requires high-efficiency desalting systems and high-efficiency solar conversion systems. RO is in the lead for high efficiency, particularly for seawater. ED can be in the lead for lower salt content sources. Photovoltaic desalination is in the lead for higher-efficiency conversion to power.
- Competitiveness is increased by:
  - RO of higher water and lower salt permeability and lower cost per unit surface
  - ED of higher current density and lower electric resistance and lower cost per unit surface
  - PV solar cells of higher standard test efficiency and higher field efficiency and lower cost per unit surface

1.5.2 Reducing CO_2 Emissions

- If fossil fuels have to be used, the solutions to lowering CO_2 emissions is to develop higher efficiency energy conversion devices and/or produce more products for the same emissions.
- Competitiveness is increased by
  - Cogeneration of power and desalted water by base-load power plants
  - Producing night low-storage-cost products to improve the load factors of power plants and of variable-load (non-base-load) cogeneration plants.

1.5.3 Desalination of Zero Liquid Discharge

- Adequate understanding of the feed saturation limits, their sequence, their dynamics of salt release and the separation of their solids are essential for the idea of zero liquid discharge.
- Membrane desalting is inherently high efficiency and cost-effective due to its avoidance of water phase change.
  - Membranes should be designed to discriminate between salt species with respect to their solubility limits. Ideally two types are needed; one membrane retains all species except sodium chloride, and the other one retains sodium chloride and stands pressures as high as 5000 psia.

  - A doping method for longer supersaturation time is needed to avoid the clogging of membrane passages.
- Vapor compression desalting pays an energy penalty for the presence of phase change but has the advantages of low-pressure operation, high biofouling resistance, and less severe clogging problems. These advantages are also desirable for zero liquid discharge
  - The vapor compressor should be made of a strong lightweight composite to run efficiently at the desired high speed with lower stresses.
  - Vapor compression intake at atmospheric pressure helps further increase the compressor efficiency and reduce its cost if scaling can be avoided.

1.6 CONCLUSIONS

Solar desalination of conventional concentration ratios has a high potential to replace fossil fuel and avoids its CO_2 emission for the production of desalted water. Supporting research to improve photovoltaic conversion efficiency and the driven desalting efficiency is worthwhile. Reverse osmosis and electrodialysis are in the lead for higher desalting efficiency.

Zero liquid discharge desalination to avoid environmental damage due to dumping of rejected brine is far from being cost effective. Further research is needed.

Reverse osmosis driven by a simple combined cycle to produce water produces much lower CO_2 emission than conventional power distillation cogeneration systems. RO driven by high-firing cooled-blade combined cycle further reduces CO_2 emission.

Power plants and cogeneration plants that burn fossil fuel and operate under variable power demand can benefit from night products of low storage cost in short supply. Night products improve the plant load factor, produce more products for the same CO_2 emission and raise profitability.

Increasing the efficiencies of conventional energy conversion devices and reducing their costs have their limits in meeting the challenge of rising fuel prices and rising CO_2 emission. New processes using new materials and new devices need to be discovered.

1.7 THE SOFTWARE PROGRAMS DEVELOPED BY THE AUTHOR FOR SYSTEM ANALYSIS

(The software discussed may be downloaded at http://booksupport.wiley.com).

1.7.1 Four Programs Developed and Their Entries

- *DesRvst*: handles the systems of the first six configurations. These are the systems of: GT/MSF, SCC, VC/SCC, VCZLD, RO/SCC, and ROZLD. Each system has its own results of states, processes and costs displayable

or printable. An overall energy balance and exergy balance verifies the consistency of the results. The program has the following entries:

- ◦ GT/MSF cogeneration systems
- ◦ Simple combined cycle systems with night RO desalter
- ◦ Simple combined cycle systems with night electrolyzer
- ◦ RO rejecting brine driven by simple combined cycle
- ◦ RO rejecting salt driven by simple combined cycle
- ◦ VC rejecting brine driven by simple combined cycle
- ◦ VC rejecting salt driven by simple combined cycle
- ◦ Change economic environment (default $25/bl)
- ◦ Change power demand profile
- ◦ Change units IP/SI (default IP)
- ◦ Change zero exergy state (default sea)

• *SOLRO*: handles PV/RO systems and has the following entries:

- ◦ Design solar-panel-driven RO system
- ◦ Run sample of up to 10 systems
- ◦ Display all results
- ◦ Print all results
- ◦ Print selected results
- ◦ Change units IP/SI (default IP)
- ◦ Change zero exergy state (default sea)
- ◦ Change economic environment (default $25/bl)
- ◦ Review software description
- ◦ Terminate

• *SOLED* handles PV/ED systems and has the following entries:

- ◦ Design solar-panels-driven ED system
- ◦ Run sample of up to 10 systems
- ◦ Display all results
- ◦ Print all results
- ◦ Print selected results
- ◦ Change units IP/SI (default IP)
- ◦ Change zero exergy state (default sea)
- ◦ Change economic environment (default $25/bl)
- ◦ Review software description
- ◦ Terminate

• *Osmosis* handles osmosis power systems and has the following entries:

- ◦ Compute one-stage osmosis given hs and dP/P

- Design one-stage osmosis given flow passages
- Display all results
- Print all results
- Print selected results
- Run sample of 10 systems given hs and dP/P
- Print sample runs
- Change Units IP/SI (default IP)
- Change zero exergy state (default sea)
- Change economic environment (default $25/bl)
- Review software description
- Terminate

1.7.2 Major Ingredients of Each Program

These ingredients are as follows:

- System description in terms of working fluids, devices, and thermodynamic decision variables
- A routine for changing decision variables manually
- Computational routine in communication with fluid thermodynamic and transport properties and with the connectivity of devices to compute a solution per a selected reference unit mass. Connectivity may be explicit (handling several configurations) or embedded in the computational routine (handling one configuration at a time). The speed of computation depends on system connectivity, system decision variables, and the complexity of the controlling equations.
- A routine to compute parameters of interest, once a solution is obtained, such as heat, power and mass rates; efficiencies; exergy destructions; costs and objective function
- For the systems shown in Figures 1.1–1.3, an optimization routine that automates the optimization of the system

1.7.3 The Software

The software developed for system analysis contains the following properties:

- Installation of the software in the user's computer is automatic.
- The software contains:
  - The chapter explained in slides
  - Executable versions of the four programs
  - The source code of their master programs
  - Sample source codes of property and process programs

APPENDIX

Some Useful Equations and Facts for Water Desalination Modeling as Employed in this Chapter [14].

1.A.1 Brief Description of the Thermodynamic Model of a System and the Design Models of Its Main Components

1.A.1.1 Thermodynamic Model The model has a database of fluid properties and elementary processes that are the building blocks of a fair number of power generation and cogeneration systems. The fluid property database contains the equations essential for computation of the thermodynamic and transport properties of H_2O, NH_3, R_{12}, and NH_3/H_2O mixtures, seven ideal gases (O_2, N_2, H_2O, CO_2, SO_2, CO and H_2) and their combination which can cover air, gas mixtures, combustion gases dry or wet; and seven liquids (lubricating oil, ethylene glycol, glycerin, kerosene, sodium, bismuth, mercury, and seawater/brines). Refrigerants R142a and R153b were also included. The process database contains 22 elementary processes that allow the description of a large number of systems. The main elementary processes handle expansion, compression, heat exchange, mixing, combustion, and throttling. Few processes are simple combinations of the elementary processes, such as a multistage process. Few are purely computational, performing tasks such as splitting, merging, and tearing. The performance of a main elementary process is described by its overall efficiency and loading parameters. More than one set of the essential input parameters is allowed by the thermodynamic model to enhance system computation with the fewest iteration loops.

The model is also used to express the exergy destruction of a device in terms of the device efficiency and loading parameters. To compute the exponents $\{n_e\}$ of a device that correlates its exergy destruction D in terms of its efficiency and loading parameters, the process model of the device is run with different input variables covering the range of interest to its system. The computed exergy destruction D is listed versus its correlating parameters. A curve-fitting procedure gives the value of $\{n_e\}$ applicable over the range of variation considered.

1.A.1.2 Sample Design Models The purpose of the following design models is to provide a rational basis for the cost of their devices. For this purpose *all* design models target the evaluation of a *dominating flow passage surface* for which a unit cost gives a fair prediction of the estimated device cost. The design models represent some of the current design practices and not necessarily the best ones. They also need to be updated to accommodate changes in design practices.

1.A.1.2.1 The Axial Air Compressor The basic features are axial, two dimensional analysis at the mean radius, subsonic, 50% reaction, diffusion factor <0.45, and ideal gas properties. Blade geometry is kept constant. All stages except the final one experience the same temperature rise. Tip blade speed, axial velocity, root/tip radius ratio, and work factors are kept constant at 1150 ft/s^{-1} (250 m/s^{-1}), 500 ft/s^{-1} (150 m/s^{-1}), 0.5, and. 0.98–0.83 (0.83 after the third stage), respectively.

A polytropic efficiency is assumed, velocity triangles computed, and the stage efficiency is evaluated from cascade tests corresponding to the blade geometry. Computations are iterated until polytropic and stage efficiencies are matched. Mass rate, pressure ratio, and temperature rise per stage are varied, and the number of stages, total surface of fixed and moving blades, adiabatic efficiency, speed, and recommended solidity are computed. An arbitrary value of solidity can also be entered as input. The total surface of the moving and fixed blades is correlated in terms of air mass flow rate, pressure ratio, and efficiency ratio $\eta/(1-\eta)$. Ambient conditions are assumed for air at compressor inlet. A version of the model accommodates low-pressure ratio *axial and radial steam compressors*.

1.A.1.2.2 The Gas Turbine The basic features are axial, uncooled blades, two-dimensional analysis at mean radius, subsonic, 50% reaction, and ideal gas properties. Blade geometry is kept constant. Loading and flow coefficients ψ,ϕ, mean blade speed, and inlet temperature are kept constant at 1.4, 0.8, 1115 ft/s (240 m/s) and 1600°F (870°C) respectively. The inlet temperature implies uncooled expansion. The first two values seem to minimize the needed total surface of blades. Stage efficiencies of nozzle and rotor blades are assumed, velocity triangles are computed, and stage and tip clearance losses are evaluated from cascade tests corresponding to the blade geometry. Computations are iterated until the assumed efficiencies and the losses are matched. Mass rate, pressure ratio, and speed are varied, and the number of stages, total surface of nozzle and rotor blades, adiabatic efficiency, and recommended solidity are computed. An arbitrary value of solidity can be entered as input. The model does not guarantee that the speed matches that of the compressor. The total blade surface of the fixed and moving blades is correlated in terms of gas flow rate, expansion ratio, and efficiency parameter $\eta/(1-\eta)$. Gas pressure at exit is assumed to be ambient.

1.A.1.2.3 The Steam Turbine The steam turbine is similar to the gas turbine except for a few differences. Actual steam properties were used to compute the specific heat and the isentropic index instead of the constant values assumed in the case of air and combustion gases. Inlet temperature and pressure and exit pressure instead of the pressure ratio became inputs. Exit pressure was changed to cover both condensing and backpressure turbines. In some cases the blade heights were too short and high rotational speeds were entered to reduce mean diameter and increase blade height. The total surface of blades did not change with the change in speed. The total surface of the blades is correlated in terms of steam mass rate, (T/P) at inlet, exit pressure, and efficiency ratio $\eta/(1-\eta)$. Impulse stages are not included.

1.A.1.2.4 Centrifugal Pumps The basic features are centrifugal, axial flow at inlet and radial flow at exit, with velocity head recovery. Loading (head) and flow coefficients Ψ, Φ, number of impeller blades, root/eye radius ratio, velocity exiting casing, specific volume, and maximum head per stage are kept constant at 1.4, 0.8, 7, 0.4, 6 ft/s (1.8 m/s), 0.016 cu ft/lb (0.001 m^3/kg), and 500 ft (150 m), respectively. Velocity triangles and flow passages are computed given specific speed.

Mass flow rate, head and specific speed are varied. Speed, surface of impeller, diffuser surface, and efficiency are computed. Specific speed is changed such that surface is minimized. One costing equation did not fit all cases. One equation was used for low flow rates and high-pressure heads (feed pumps) and one for large flow rates and low-pressure heads (circulating pumps). Extending flow rates to > 500 lb/s need to be implemented. Impeller surface is correlated in terms mass rate, pressure head, and efficiency ratio $\eta/(1-\eta)$.

1.A.1.2.5 Gas Turbine Combustor The basic features are annular tube and burning natural gas. Inlet and exit temperatures, air/fuel mass ratio, and number of cans are kept constant at 1600°F (870°C), 500°F (260°C), at values of 75, and 7, respectively. Air mass rate, pressure, and pressure loss are varied and the combustor surface computed. (60 m/s). The maximum velocity was set at 200 ft/s. Combustion intensity varied at ~80 kW $(\text{ft}^3 \cdot \text{atm})^{-1}$ (2000 kW $(\text{m}^3 \cdot \text{atm})^{-1}$). The combustor surface is correlated in terms air mass rate, inlet pressure, and pressure loss.

1.A.1.2.6 Heat Exchangers The basic features are forced convection heat exchange, single- and two-phase fluids, and three generic types of exchangers (double-tube, fin-plate, and shell-and-tube). For the shell-and-tube type, flow may be counter or crosscounter, tubes may be plain or finned on the outside, and shell may be cylindrical or duct-type. In two-phase procedures, more than one equation is used for film coefficients and friction factor multipliers. Pressure losses were based on the worst-case multiplier. The plate-fin type consists of layers of plates with straight parallel fins on each side of each plate. The fins on one side are perpendicular to those of the other side. Two sets of layers may be connected in series to allow for mixing. A surface geometry is selected. For shell and tube geometry, tube length, diameter, and pitches, and shell diameter or width and depth are entered. For the plate-fin geometry, the number of plates, fins per inch on either side, and their heights and thickness are entered. Two groups of boundary parameters can be entered: mass rates and temperature and pressures at all inlets and exits or mass rates and inlet pressures and temperatures and effectiveness. With both entries, film coefficients of heat transfer and pressure drops are computed. The heat exchange surface is computed in either of two ways: surface by geometry or surface $= Q/U\,\Delta T$. With the first entry computations are iterated until the two areas are matched and the two pressure drops are accommodated. With the second one, only the surface iteration is needed. The pressure drops are output parameters. The iterations are both manual and automated to minimize the heat exchange surface. This program, evolved in parallel with the thermodynamic model.

The superheater, the boiler, and the economizer of the heat recovery steam generator assumed duct- type shell and tubes with outside circular fins. Fin geometry on the outside of the steam generator tubes and fouling factors in heat exchange are kept constant. The brine heater and the flash stages are assumed to have plain tubes. The brine heater is assumed to have a cylindrical shell. The flash stages are assumed to have a duct-type shell. A constant temperature drop is assumed for all the stages and a chamber at a temperature of 150°F (65°C) is assumed to represent

all the stages. A heat transfer temperature difference correction is introduced for the rejection stages. Two types of air preheater are considered: shell-and tube with circular fins on the outside or a plate-fin type. For the evaporator/condenser a vertical shell-and-tube type with plain tubes is assumed. The heating steam condenses in the tubes, and the liquid is sprayed on the outside at a rate 10 times the vaporized liquid. In all the exchangers fouling factors are kept constant. Inlet parameters are varied. The temperature profile is first computed and checked for crossings and pinch point. Rate of heat exchange, effective temperature difference of heat transfer, and heat exchange surface are computed among other detailed heat transfer outputs. Pressure drops, if outputs, are computed. Given the inlet pressure temperature and mass rate for the two fluids, all heat exchange surfaces are correlated in terms the rate of heat exchange, a temperature difference (terminal or logarithmic mean) and hot and cold side pressure losses. In a flash stage, any temperature drop induced by flashing is used instead of a pressure loss. The effect of pressure and temperature levels is accounted for in the unit cost (severity of operation).

1.A.1.2.7 Radiant Heat Exchange in Boiler A simple model is assumed. The basic features are square vertical duct type, forming water walls combined with reflectors and backed with insulation. The water boils in the tubes, and the vapor formed is separated in an upper drum. The total radiation exchange between the entire gas volume and the walls is based on the mean beam length. The absorption bands of H_2O and CO_2 of the hot gases are factored in. The effect of temperature variation along the duct is accounted for by dividing the gas path into five sections, each with a uniform temperature. The gas is assumed to enter at the adiabatic flame temperature. The effect of convective film coefficients and wall resistance is included. The height of the duct and its width were observed to control both the gas-side and the steam-side pressure losses, beside the heat exchange surface. The gas-side pressure loss was not significant because of the significant change in gas temperature and the associated lowering of gas velocities. The tube-side pressure drop progressively increased as the height is increased relative to the width with negligible effect on the heat transfer coefficient. The heat exchange is expressed by an overall heat transfer coefficient ranging from 30 to 50 Btu $(h \cdot ft^2 \cdot F)^{-1}$ [0.170–0.284 kW $(m^2 \cdot K)^{-1}$], while convection-induced heat exchange was lower by only one order of magnitude. The surface of the wall tubes is correlated in terms of the rate of heat transfer and the conventional logarithmic mean temperature difference. An equivalent temperature driving force $\Delta T_r = (T_{gas}/T_{flame})^4 - (T_{steam}/T_{flame})^4$ was used in earlier applications with a different correlation ($A = 0.39Q\,\Delta T_r^{-2}$).

1.A.1.2.8 Curve-Fitting Costing Equations and Exergy Destruction Various mathematical procedures are available for curve fitting by minimizing the deviations around a fit. The number of the surfaces A or exergy destructions D generated should be much larger than the correlating parameters, which usually vary from 2 to 4. One simple procedure is to use sets of number equal to the number of the correlating parameters plus one, to obtain the coefficient k and exponents $\{n\}$. The

ratios of the computed A generated by a set to the corresponding one generated by the design model are computed. The process is repeated with different sets until a set is found where the ratios deviate the least from one. The same rule of thumb applies to D. The correlating parameters of the costing equations and their range of applicability are given in Section 1.A.2.

Deviations in curve fitting were within $\pm 10\%$, and in very few cases of a wide range of applicability deviations of $\pm 20\%$ were found. It is important to note that improved correlations depend on improving the quality of models and reducing their range of applicability.

References listed in Section 1.F.10 at the end of this chapter are additional useful readings for the preceding Section 1.A.1.

1.A.2 The Capital and Fuel Costing Equations of some common Devices (Tables 1.A.1 and 1.A.2)

For illustration, let the device be a forced-convection heat exchanger. It is assumed to be the superheater, component 7 of the heat recovery steam generator of the simple combined cycle of Figure 2. A duct shell-and-finned tube type is assumed. The fins are assumed circular on the outside that is, on the gas side. The design model of heat exchangers described in Secion 1.A.2 is used.

The boundary parameters P, T, $\{x\}$, M at inlets and exits of the exchanger as embedded in the system at a design point for the system are used. The exchanger physical surface and its geometry are defined by length, diameter, spacing, number, material, material thickness and fin geometry of the tubes. These parameters are usually more than sufficient to allow for adjustment to match the computed surface and pressure drops by film coefficients and friction factors for the given heat load and its temperature profile. Any extra design degrees of freedom are used to minimize the surface and/or to satisfy reliable design practices. The design process is thus a matching/minimizing process.

The minimized surface as a function of performance is generated by repeating this design process for different boundary parameters within a range relevant to the optimization of the system. A specific geometry of minimized surface is obtained for each set of boundary parameters. The surface is then expressed by an appropriate set of performance parameters such as heat loads, mass rates, heat exchange temperature differences, effectiveness, and pressure losses. In this example, the surface of the fins and tubes is expressed in terms of the heat load, the logarithmic mean temperature difference and pressure losses on the shell side and on the tube side. The following form is used:

$$A = kQ^{n1}\Delta T_m{}^{n2}\Delta P_t^{n3}\Delta P_s{}^{n4} \tag{1.A.1}$$

where A is converted to a costing equation by

$$Z = c_a A \tag{1.A.2}$$

Table 1.A.1 Generated Capital Costing Equations and Their Local Objectives

	Costing Equation $Z = c_a A\ A = kx_1^{n1}x_2^{n2}x_3^{n3}x_4^{n4}$			Local Objective $J(Y) = c_d\ D + c_z Z = KeY^{ne} + k_z Y^{nz}$			
Device	c_a \$k/ft^2 /(m^2)	k, IP/(SI)	$x_1^{n1}x_2^{n2}x_3^{n3}x_4^{n4}$ ranges of $\{x\}$,(IP/SI)	Y	n_e	n_z	Dissipation
1 Axial compressor	50 (538)	0.15 (0.0063)	$M^1\ \mathrm{Pr}^{0.45}\ e^{0.45}$ 50–1000, 5–15, 2.3–11.5 (25–455, 5–15, 2.3, 11.5)	e	−0.95	0.45	D_{PT}
2 Gas turbine	50 (538)	0.32 (0.0135)	$M^1\mathrm{Pr}^{-0.5}e^{0.85}$ 50–1000, 5–15, 4–19 (25–455, 5–15, 4–19)	e	−0.8	0.85	D_{PT}
3 Steam turbine	50 (538)	0.9 (1.978)	$M^1(T_i/P_i)^{0.05}P_e^{-0.75}e^{0.9}$ 25–100, 1.5–30, 1–150, 4–19 (11–45, 120–2400, 0.0071–1.03, 4–19	e	−0.8	0.90	D_{PT}
4 Pump feed	3 (32)	0.0025 (0.000435)	$M^{0.55}\Delta P^{0.55}e^{1.05}$ 5–70, 14–900, 1.8–9 (2–32, 100–6200, 1.8–9)	e	−1	1.05	D_{PT}
5 Pump cooling-water	3 (32)	0.0063 (0.00183)	$M^1\Delta P^{0.1}e^{0.7}$ 100–500, 2–25, 4–14 (45–230, 14–170, 4–14)	e	−1	0.7	D_{PT}
6 Fan/blower	3 (32)	0.063 (0.0183)	$M^1\Delta P^{0.1}e^{0.7}$ 100–500, 0.1–0.6, 2–9 (45 = 230, 0.7–4, 2–9)	e	−1	1.05	D_{PT}
7 Combustor	0.2 (2.15)	5.85 (0.261)	$M^{0.5}P^{0.24}dp^{-0.75}$ 400–900, 50–200, 0.01–0.3 (180–410, 0.34–1.38, 0.01–0.3)	dP	1	−0.75	D_P

(*Continued*)

Table 1.A.1 (*Continued*)

	Costing Equation $Z = c_a A\ A = k x_1^{n1} x_2^{n2} x_3^{n3} x_4^{n4}$			Local Objective $J(Y) = c_d D + c_z Z = K e Y^{ne} + k_z Y^{nz}$			
Device	c_a \$k/ft^2 /(m^2)	k, IP/(SI)	$x_1^{n1} x_2^{n2} x_3^{n3} x_4^{n4}$ ranges of $\{x\}$,(IP/SI)	Y	n_e	n_z	Dissipation
8 Superheater, convective	0.03 (0.32)	340 (32.48)	$Q^1 \Delta T_m^{-1} dP_t^{-0.15} dP_s^{-0.14}$	ΔT_m	1	−1	D_T
			10–15, 100–200, 6–13, 0.06–0.44	dP_t	1	−0.15	D_{PT}
			(10–15, 55–110, 40–90, 0.4–3)	dP_s	1	−0.14	D_{Ps}
9 Boiler, convective	0.03 (0.32)	340 (32.48)	$Q^1 \Delta T_m^{-1} dP_t^{-0.33} dP_s^{-0.26}$	ΔT_m	0.45	−1	D_T
			(25–55, 75–200, 6–13, 0.06–0.44	dP_t	1	−0.33	D_{PT}
			25–55, 40–110, 40–90, 0.4–3	dP_s	1	−0.26	D_{Ps}
10 Economizer	0.03 (0.32)	310 (29.89)	$Q^1 \Delta T_m^{-1} dP_t^{-0.16} dP_s^{-0.125}$	ΔT_m	0.45	−1	D_T
			15–40, 70–105, 6–26, 0.007–0.56	dP_t	1	−0.16	D_{Pt}
			15–40, 38–60, 40–180, 0.5–4	dP_s	1	−0.125	D_{Ps}
11 Brine Feed heater condenser	0.04 (0.43)	3.3 (0.367)	$Q^1 \Delta T_t^{-0.7} dP_t^{-0.08} dP_s^{-0.04}$	ΔT_t	0.9	−0.7	D_T
			40–185, 5–15, 0.1–7, 0.001–1.3	dP_t	1	−0.08	D_{PT}
			(40–185, 2.5–80, 0.7–50, 0.007–9	dP_s	1	−0.04	D_{Ps}
12 MSF	0.04 (0.43)	10 (1.6)	$Q^1 \Delta T_n^{-0.75} \Delta T_t^{-0.5} dP_t^{-0.1}$	ΔT_n	1.5	−0.75	D_T
			14–110, 3–10, 3–12, 0.2–10	ΔT_t	1	−0.5	D_T
			14–110, 1.7–6, 1.7–7, 13–70	dP_t	1	−0.1	D_{Pt}
13 Radiant boiler	0.08 (0.86)	100 (16.73)	$Q^1 \Delta T_m^{-1}$				
			50–600, 0.1–1	$dP_t = 0.0004A - 25$ $dP_t = 0.000037A - 1.72$	No tradeoffs; dependent on surface		

14 Air Preheater plate-fin	0.008 (0.086)	37,000 (3496)	$Q^1 \Delta T_m^{-2} dP_h^{-0.3} dP_c^{-0.3}$	ΔT_m	1	−2	D_T
			10–100, 50–150, 0.03–1.5, 0.03–1.5	dP_h	1	−0.3	D_{Ph}
			(10–100, 28–83, 0.2–10, 0.2–10)	dP_c	1	−0.3	D_{Pc}
15 Air Preheater shell-and-tube	0.03 (0.32)	2750 (235)	$Q^1 \Delta T_m^{-1.5} dP_t^{-0.3} dP_s^{-0.2}$	ΔT_m	1	−1.5	D_T
			10–100, 50–150, 0.03–1.5, 0.03–1.5	dP_t	1	−0.3	D_{Ph}
			(10–100, 28–83, 0.2–10, 0.2–10)	dP_s	1	−0.2	D_{Pc}
16 Throttle valve	0.75 (8.07)	0.45 (0.989)	$M^1 (T_i/P_i)^{0.05} P_e^{-0.75}$	No tradeoff			
			5–20, 1.5–5, 0.5–100				
			(2–9, 120–400, 0.003–0.7)				
17 Mixing chamber	30 (1060)	1 (1)	V^1	No tradeoff			
18 c_a pressure factor	—	0.191 (0.85)	$P^{0.3}$	No tradeoff			
19 Evaporater condenser	0.04	6.2	$Q^1 \Delta T_m^{-1} dP_t^{-0.01} dP^{-0.1}$	ΔT_m	1	−1	D_T
			150–800, 4–40, 0.01–0.05, 0.01–0.04	dP_t	1	−0.01	D_{Ph}
			(50–800, 2–22, 0.06–0.35, 0.06–0.3	dP_s	1	−0.1	D_{Pc}
20 Vapor Compressor, radial	9 (96.9)	0.0018 (0.000076)	$(v\ M)^1\ Pr^1\ e^{0.7}$	e	−0.95	0.7	D_{PT}
			M50–1000, 1.1–2, 2.3–11.5				
			(M22–455, 1.1–2, 2.3–11.5)				
21 *hx* general approximation	0.04	5	$Q^1 \Delta T_m^{-1} dP_t^{-0.15} dP_s^{-0.15}$	ΔT_m	−1	0.5	D_T
			15–100, 4–40, 0.05–1, 0.03–0.4	dP_t	1	−0.15	D_{Ph}
			(15–100, 2–22, 0.3–7, 0.2–2.3)	dP_s	1	−0.15	D_{Pc}

Notations: In columns 2–4, Imperial (UK) values are presented First, Followed by SI (intemational; metric) values in parentheses. Imperial (IP) units: c_a, \$$k$/ft^2; A, ft^2; M, lb/s; Q, kW (range MW); P_i, P_e, psia; T_i, R; ΔT, °F;
$\Delta P, dP$, psi; V, ft^3/s. SI units: c_a, \$k/m^2; A, m^2; M, kg/s; Q, kW (range MW); P_i, P_e, MPa; T_i, K; ΔT, °C;
$\Delta P, dP$, kPa; V, m^3/s. Nomenclature: D = dissipation (exergy destruction), kW; $D = D_P + D_T + D_C$, $D_{PT} = D_P + D_T$; c_d = unit cost of exergy destruction, \$/kWh, $e = \eta/(1-\eta)$; Pr = pressure ratio. General notes: Effect of pressure on unit costs is assumed 1 for pressures < 250 psia; cost of a steam ejector is assumed double that of the throttle valve.

Table 1.A.2 Generated and Gathered Off-Design Performance Equations

Component	Equations
	By Design Models
6) Combustor	$\Delta P = \Delta P_d (M_g/M_{gd})^{1.75}$
7) Superheater	$\eta = \eta_d (M_h/M_{hd})^{0.2} (M_c/M_{cd})^{-0.15}$
	$\Delta P_h = \Delta P_{hd} (M_h/M_{hd})^{1.75}$
	$\Delta P_c = \Delta P_{cd} (M_c/M_{cd})^{1.8}$
8) Boiler	$\eta = \eta_d (M_h/M_{hd})^{-0.05} (M_c/M_{cd})^{0.01}$
	$\Delta P_h = \Delta P_{hd} (M_h/M_{hd})^{1.75}$
	$\Delta P_c = \Delta P_{cd} (M_c/M_{cd})^{1.75}$
9) Economizer	$\eta = \eta_d (M_h/M_{hd})^{0.15} (M_c/M_{cd})^{-0.05}$
	$\Delta P_h = \Delta P_{hd} (M_h/M_{hd})^{1.75}$
	$\Delta P_c = \Delta P_{cd} (M_c/M_{cd})^{1.1}$
10) Condenser	$\eta = \eta_d (M_h/M_{hd})^{-0.05} (M_c/M_{cd})^{-0.35}$
	$\Delta P_h = \Delta P_{hd} (M_h/M_{hd})^{1.41}$
	$\Delta P_c = \Delta P_{cd} (M_c/M_{cd})^{0.6}$
	By Generalized Correlations
11) Compressor (axial)	$M_r = M/M_d$
	$\eta_r = a_1 + a_2 M_r + a_3 M_r^2$
	$M_r \geq 0.5, \eta_r = 0.9$
	$\eta = \eta_d \eta_r / \eta_{rd}$
	$PR = PR_d M_r$
12) Adjustable IGV	$a_1 = -0.7508, a_2 = 3.2414, a_3 = -1.5906$
Adjustable IGV + 5 stators	$a_1 = 0.3337, a_2 = 1.0917, a_3 = -0.5254$
Gas turbine	$PR_r = PR/PR_d, M_r = N_M/N_{Md}$
	η_r or $M_r = (a_1 + a_2 PR_r + a_3 PR_r^2)$
	$N_M = M/P(T)^{0.5}$, a correlating flow number
	$\eta = \eta_d \eta_r / \eta_{rd}$
	$\eta_{rd} = 0.9, a_1 = 0.6164, a_2 = 0.6179, a_3 = -0.3343$
	For $PR_r \geq 0.53, M_r = 1$
	For $PR_r < 0.53, M_r$ has
	$a_1 = 0.1228, a_2 = 2.8283, a_3 = -2.2145, T_{firing} =$
	$(M_r N_{Md} P_i / M_{air})^2$ to match rpm (r/min)
Steam turbine	$M_r = M/M_d, PR_r = PR/PR_d$
	$\eta/\eta_d = A_1 + A_2 M_r + A_3 M_r^2$
	$A_i = a_{i1} + a_{i2} PR_r + a_{i3} PR_r^2$
	Reaction turbine $a_{ij} =$
	0.247917, 0.128125, −0.0101042
	1.23125, −0.221875, 0.0215625
	−0.479167, 0.09375, −0.0114583
	Impulse turbine $a_{ij} =$
	0.425833, 0.001875, 0.00302083
	0.882500, 0.066875, −0.01031250
	−0.308333, −0.068750, 0.00729167
Feed pump	$M_r = M/M_d, \Phi_r = 0.1$
	$\Psi_r = 0.52, \eta_r = 0.85$
	$\Phi = \Phi_r M_r, \Phi \leq 0.15$
	$\Psi = 0.595 - 0.3\Phi - 4\Phi^2$
	$\eta = (14\Phi - 56.9\Phi^2)/\eta_r \eta_d$
	$P = P_d \Psi / \Psi_r$
Cooling-water pump	$M_r = M/M_d, \Phi_r = 0.13,$
	$\Psi_r = 0.3, \quad \eta_r = 0.9$
	$\Phi = \Phi_r M_r, \Phi \leq 0.18$
	$\Psi = 0.55 - 1.83\Phi - 0.667\Phi^2$
	$\eta = (12.167\Phi - 43.3\Phi^2)/\eta_r \eta_d$
	$P = P_d \Psi / \Psi_r$

The unit cost c_a depends on the type of material and the manufacture process and is also dependent on time and location. It is expressed thermodynamically as function of pressure, temperature and composition (severity of operation). In this example, c_a is assumed per unit total surface of fins and tubes. Ten minimized surfaces were generated by changing inlet P, T and M; the allowed pressure losses and effectiveness were also included. Heat load, exit conditions, and logarithmic mean temperature difference are recorded. The parameters that remain fixed are the fin geometry, tube thickness, tube arrangement (staggered), fouling factors, flow directions (gas horizontal, steam with gravity). In this particular example, the effect of gravity on pressure losses is negligible. Table 1.A.3 lists the recorded parameters of the 10 minimized surfaces and the quality of the correlation.

The constant k and the four exponents n_1, n_2, n_3 and n_4 of Equation (1.A.1) are computed by using the surfaces of five cases simultaneously. These five cases are selected randomly from the total number of cases. The computed constant and exponents that best fit the surfaces of all the cases is selected. The simultaneous solution involves the inverse of a 4×4 matrix. When the matrix determinant is relatively small, unreasonable exponents are obtained and have to be rejected. Also, some selections may give rise to singular solutions and fail to give any values altogether. There are, however, many sets that give solutions. There is also opportunity to round off the best-fit exponents along with a modified value of the constant k such that the quality of the fit is not changed. The best fit is selected by comparing various sets. No formal regression approach is used to seek the best fit.

The constant and exponents obtained were $k = 30.71, n_1 = 1, n_2 = -1$, $n_3 = -0.15$, and $n_4 = -0.14$. The equation is applicable in the range $Q = 8$ to 66 MW, $\Delta T_m = 38$ to 130°C, $\Delta P_t = 20$ to 90 kPa, and $\Delta P_s = 0.2$ to 1.2 kPa with average scatter $\pm 8\%, \max +10\%$. Inside tube surfaces covered the range 110 to 975 m^2.

1.A.3 Some Useful Forms of Flow Exergy Expressions

1.A.3.1 Equations

$$E = H - T_0 S - \sum \mu_{i0} X_i \tag{1.A.3}$$

where E is the flow exergy per unit matter. Then we can, either use

$$[H_{0d} - T_0 S_{0d}]_{T_0, P_0, \{Xi_0\}} = \sum \mu_{i0} X_i \tag{1.A.4}$$

or introduce

$$[H_0 - T_0 S_0]_{T_0, P_0, \{Xi\}} = \sum \mu_i X_i \tag{1.A.5}$$

Equation (1.A.4) uses the dead-state enthalpy and entropy directly by the subscript od. Equation (1.A.5) introduces an intermediate state at T_0, P_0 without changing

Table 1.A.3 The Superheater Performance/Design Correlating Matrix Minimized Surfaces Versus Thermodynamic and Geometric Parameters

Run	A_{tube} m^2	Q, MW	ΔT_{lm}, °C	η	ΔP_t, kPa	ΔP_s, kPa	L_{tube}, m	d_o, cm	W_{sh}, m	Pitches 1, 2, cm		A_{fin}/A_i	N_{tube}	N_{pass}
1	486	15.76	66	0.921	42	0.462	20.4	2.5	11.9	5	4.52	11.8	364	1
2	915	66.80	128	0.609	41	0.475	5.8	2.5	52.1	5	4.52	11.8	2,397	2
3	620	17.32	49	0.883	42	0.544	29.6	2.5	8.8	5	4.52	11.8	321	1
4	897	31.50	66	0.921	48	0.627	20.4	2.5	20.4	5	4.52	11.8	673	1
5	856	34.66	66	0.921	37	1.192	16.8	2.5	20.1	5	4.52	11.8	776	1
6	976	34.28	39	0.921	82	0.903	12.2	5	15.5	10	9.04	19.7	1,258	8
7	188	7.88	66	0.921	90	0.834	85.3	7.6	0.91	15	13.6	27.8	10	1
8	276	8.67	66	0.921	90	0.227	45.7	3.8	3.7	7.6	6.78	15.7	57	1
9	355	9.52	66	0.919	21	0.234	29.6	3.8	6.4	7.66	0.78	15.7	114	1
10	112	9.52	126	0.400	83	0.965	34.1	7.6	2.1	15	13.6	27.8	15	1
						Scatter of the Correlating Costing Equation								
Run			1	2	3	4	5	6	7	8		9	10	
A_{eqn}/A_{table}			0.965	1.10	1.08	0.98	1.06	0.92	1.02	0.92		0.976	1.08	

composition using the subscript o. In fact, any intermediate state convenient for property computations can be introduced. Using Equation (1.A.5), we obtain

$$E = (H - H_0) - T_0(S - S_0) + \sum(\mu_i - \mu_{i0})X_i \tag{1.A.6}$$

where the thermal mechanical part of exergy is

$$E^{\mathrm{tm}} = (H - H_0) - T_0(S - S_0) \tag{1.A.7}$$

and the chemical part is

$$E^{\mathrm{c}} = \sum(\mu_i - \mu_{i0})X_i \tag{1.A.8a}$$

$$= \mathrm{R}T_0 \sum X_i \ln\left(\frac{a_i}{a_{i0}}\right) \tag{1.A.8b}$$

where

$$a_i = \gamma_i X_i = \frac{f_i}{f^0} \tag{1.A.9}$$

- *For Ideal-Gas Mixtures*. The Thermal Mechanical component may be further divided into the Thermal part:

$$E^{\mathrm{t}} = C_{\mathrm{p}}(T - T_0)\left(\frac{1 - T_0}{T_{\mathrm{m}}}\right) \tag{1.A.10}$$

where

$$T_{\mathrm{m}} = \frac{T - T_0}{\ln(T/T_0)} \tag{1.A.11}$$

and the Mechanical part

$$E^{\mathrm{m}} = RT_0 \ln\left(\frac{P}{P_0}\right) \tag{1.A.12}$$

In terms of mole fractions, the Chemical part becomes

$$E^{\mathrm{c}} = RT_0 \sum X_i \ln\left(\frac{X_i}{X_{i0}}\right) \tag{1.A.13}$$

- *For Nonideal Mixture Excess Gibbs Function*

$$G_x = RT \sum N_i \ln \gamma_i \tag{1.A.14}$$

Differentiation gives

$$\gamma_i = \frac{(\partial G_x / \partial N_i)}{(RT)} \tag{1.A.15}$$

$$H_x = -T^2 \times \partial \left(\frac{G_x}{T} \right) / \partial T \tag{1.A.16}$$

$$S_x = (H_x - G_x)/T \tag{1.A.17}$$

$$V_x = \partial G_x / \partial P \tag{1.A.18}$$

- *Changes in Terms of Measurables*

$$dh = C_{\mathrm{p}} dT + [V - T(\partial V / \partial T)_{\mathrm{p}}) dP] \tag{1.A.19}$$

$$dS = C_{\mathrm{p}} \frac{dT}{T} - \left(\frac{\partial V}{\partial T} \right)_{\mathrm{P}} dP \tag{1.A.20}$$

$$f^{\mathrm{vi}} = \phi_i Y_i P \tag{1.A.21}$$

$$f^{\mathrm{li}} = \gamma_i X_i P_{\mathrm{si}} \phi_{\mathrm{si}} F \tag{1.A.22}$$

$$F = \exp \left(\int \frac{V^{\mathrm{li}} dP}{RT} \right) \tag{1.A.23}$$

$$f^{\mathrm{vi}} = f^{\mathrm{li}} \tag{1.A.24}$$

- *Two-Component Mixture, the Gibbs Excess Function is*

$$G_x = X_1 X_2 [A + B(X_1 - X_2)] \tag{1.A.25}$$

$$\ln \gamma_1 = \frac{[(A + 3B) {X_2}^2 - 4B {X_2}^3]}{RT} \tag{1.A.26}$$

$$\ln \gamma_2 = \frac{[(A - 3B) {X_1}^2 + 4B {X_1}^3]}{RT} \tag{1.A.27}$$

where A and B are particular constants for the two components

- *Using More than One Dead-State Composition*

$$\sum (\mu_i - \mu_{i0}) X_i = \sum_{i1} (\mu_i - \mu_{i0}) X_i + \sum_{i2} (\mu_i - \mu_{\mathrm{ir}}) X_i + \sum_{i2} (\mu_{\mathrm{ir}} - \mu_{i0}) X_i \tag{1.A.28}$$

Another dead state, denoted here with the subscript ir (e.g., sea), is assumed for species (e.g., salts) having traces in the usually assumed dead state denoted here with the subscript io (e.g., air) but is relatively abundant in ir. The last term is a constant of no interest in exergy change beyond the dead state ir.

- *Introducing Known Intermediate Chemical Changes*

$$\Delta G_{\mathrm{R}} = \sum_{\mathrm{R}} (\mu_i - \mu_{i0}) X_{i\mathrm{R}} - \sum_{\mathrm{P}} (\mu_i - \mu_{i0}) X_{i\mathrm{P}} \tag{1.A.29}$$

Let μ_j be a reactant (e.g., a hydrocarbon fuel) of minute equilibrium mole fraction in the assumed dead state (e.g., air); then μ_{j0} is determined by

$$(\mu_j - \mu_{j0}) X_j = \Delta G_{\mathrm{R}} + \sum_{\mathrm{P}} (\mu_i - \mu_{i0}) X_{i\mathrm{P}} - \sum_{\mathrm{R}} (\mu_i - \mu_{i0}) X_{i\mathrm{R},i\neq j} \tag{1.A.30}$$

1.A.3.2 Balances

1.A.3.2.1 Exergy Balance

$$\sum_{\text{in}} \mathrm{E_b} = \sum_{\text{out}} E_{\mathrm{b}} + \sum D \tag{1.A.31}$$

where

$$D = \text{exergy destruction} \tag{1.A.32}$$

$$E_{\mathrm{b}} = E^{\mathrm{q}} + E^{\mathrm{w}} + E^{\mathrm{f}} \tag{1.A.33}$$

$$E^{\mathrm{q}} = Q(1 - \mathrm{T}_0/\mathrm{T_b}) \tag{1.A.34}$$

$$E^{\mathrm{w}} = W_{\mathrm{s}} \tag{1.A.35}$$

$$E^{\mathrm{f}} = ME$$

1.A.3.2.2 Entropy Balance

$$\sum_{\text{out}} \mathrm{S_b} - \sum_{\text{in}} S_{\mathrm{b}} = S^{\mathrm{cr}} \tag{1.A.36}$$

where

$$S_{\mathrm{b}} = S^{\mathrm{m}} + S^{\mathrm{q}} \tag{1.A.37}$$

$$S^{\mathrm{q}} = Q/T_{\mathrm{b}} \tag{1.A.38}$$

$$S^{\mathrm{m}} = MS \tag{1.A.39}$$

$$D = T_0 S^{\mathrm{cr}} \tag{1.A.40}$$

1.A.3.2.3 A Note on the Dead State Environment An absolute dead state of zero exergy does not exist, but a reference one can be set. Arbitrary reference states have long been used. In thermodynamic properties zero enthalpy and entropy differ for different working fluids. In chemical reactions, elements are selected as reference to compute the energy and free energy of formation of compounds.

A reference dead state for zero exergy is defined by a pressure P_0, a temperature T_0 and a set of chemical species of composition $\{X_{\mathrm{io}}\}$ suitable for analyzing the utilization of energy in a particular situation. The composition $\{X_{\mathrm{i0}}\}$ is preferred to resemble a natural state in which the chemical species of interest are not traces in order to establish chemical exergies. Atmospheric air is an appropriate dead state to use for work with a number of gases, including combustion products, although the pure species may be used as reference. Seawater is appropriate for work with desalination. Bauxite is appropriate when dealing with the purification of aluminum. More than one dead state may be assigned as shown by equation (26), so long the potential work between the two dead states is not of immediate interest.

A selected dead state implies a large environment of constant values for P_0, T_0 and $\{X_{i0}\}$. In most natural environments, P_0 and $\{X_{i0}\}$ remain more or less constant but T_0 may exhibit daily and seasonal variations. When the change has significant effect on the value of exergy, exergy analysis is repeated as function of time periods of different dead state temperatures.

1.A.4 Theoretical Separation Work Extended to Zero Liquid Discharge

Theoretical work of separation may shed light on the thermodynamics and partly on the economics of zero liquid discharge. Conventional desalination approximately doubles the dissolved salt concentration of the feed. In other words, conventional desalination produces half of the feed as does desalted water product. Zero liquid discharge produces all the water in the feed as desalted water product. A theoretical work about double that of conventional desalination would hence be encouraging to the idea of zero liquid discharge.

The thermodynamic computations here assume sodium chloride as the ideal solution. Deviations from ideal solution are expected as concentration increases and the theoretical work is expected to be even higher.

Assuming an ideal NaCl solution, let X = mass fraction and x = mole fraction, $T = 80^{\circ}\mathrm{F}$. We can then calculate the theoretical power at infinite feed per unit product as follows:

$$w_{\min} = \left(\frac{\partial \mathrm{G}}{\partial \mathrm{M_w}}\right)_{\mathrm{feed}=\infty} = \mathrm{RTln}\left(\frac{1}{x_{\mathrm{w}}}\right) \tag{1.A.41a}$$

X	x	w_{min} Btu/lb pure, feed $= \infty(x_b \approx x_f)$ $RT\ln(1/x_w) \approx RTx_s (x_s \leq 0.3)$	
0.95	0.854	115	50.90
0.75	0.480	39.0	28.61
0.50	0.235	16.0	14.00
0.28	0.1069	6.74	6.37
0.27	0.1022	6.42	6.09
0.25	0.0930	5.82	5.54
0.15	0.0515	3.15	3.07
0.07	0.0226	1.37	1.35
0.04	0.0127	0.76	0.76
0.035	0.0114	0.68	0.68

The theoretical work with finite feed per unit product is obtained by integrating equation (1.A.41a) from initial x_f to final concentration x_b:

$$w_{min} = \frac{1}{M_w}\int_{x_f}^{x_b} \frac{\partial G}{\partial M_w} dM_w = \frac{RT}{M_w}\int_{x_f}^{x_b} \ln\left(\frac{1}{x_w}\right) dM_w$$

Integrating and noting that $dM_w = d(M_f(x_b - x_f)/x_b) = M_f x_f dx_b/x_b^2$ and letting $\ln(1/x_w) = x_b$ we obtain

$$w_{min} \approx \frac{RTx_b x_f}{(x_b - x_f)} \ln\left(\frac{x_b}{x_f}\right) \qquad \text{(given } M_f \text{ and } x_f\text{)} \qquad (1.A.42)$$

The theoretical work of separation taking in consideration the saturation limits of the salt species are a consequence of water separation by equation 1.A.42 for an ideal concentrator and of water and salt separation [obtained by Eq. (1.A.42)] in an ideal crystallizer.

The theoretical work taking in consideration the saturation salt content of NaCl at $80^\circ F = 0.27 lb_s/lb_{soln}$, is obtained as follows. From feed X_f to $X_{sat} = 0.27$, Equation (1.A.42) applies, producing M_{d1}. The work of salt separation in an actual process requires a departure from saturation. Letting the departure for estimating the theoretical work be zero, meaning an infinite feed of equation (1.A.41a), we obtain

$$w_{smin} \approx RTx_{sat} \qquad (1.A.41b)$$

The separated water and separated salt occur at the same x_{sat}; this means that

$$M_s/(M_{d2} + M_s) = x_{sat}$$

where M_{d2} is determined by the separated salt and vice versa.

For a given feed M_f

$$W_{min,Mf} \approx M_{d1} RTx_{sat} \frac{x_f}{(x_{sat} - x_f)} \ln\frac{x_{sat}}{x_f} + M_{d2} RTx_{sat} \qquad (1.A.43a)$$

where

$$M_{d1} = M_f(x_{sat} - x_f)/x_{sat}$$
$$M_{d2} = M_s(1 - x_{sat})/x_{sat}$$

Per unit product water

$$w_{min} = \frac{W_{min,Mf}}{M_f - M_f x_f} \tag{1.A.43b}$$

Four initial and final concentrations lb_s/lb_{soln} of NaCl aqueous solution are of interest to saline water desalination:

X_f	x_f	X_{sat}	x_{sat}	X_b	x_b	
0.035	0.0114	—	—	0.07	0.0226	represents conventional seawater desalting
0.035	0.0114	0.270	0.1022	1.00	1.00	represents ZLD seawater desalting
0.070	0.0226	0.270	0.1022	1.00	1.00	represents ZLD retrofit seawater desalting
0.250	0.0930	0.270	0.1022	1.00	1.00	represents ZLD oil field water desalting

At $T = 80^\circ F$	Per lb feed eqn (3)			Per/lb product Eq. (1.A.43b)	
M_{d1}	W_{min}	M_{d2}	$W_{s,min}$	w_{min}	
1	0.94	0	0	$0.94/1.00 = 0.94$	usual seawater desalting
0.8704	1.68	0.0945	6.092	$2.03/0.965 = 2.1$	ZLD seawater desalting
0.7407	2.61	0.189	6.092	$3.09/0.930 = 3.3$	ZLD retrofit seawater
0.0741	5.81	0.675	6.092	$4.54/0.750 = 6.1$	ZLD oil field water

The preceding theoretical analysis shows the trend of desalination theoretical energy requirement in terms of the salt content of the feed and the reject assuming

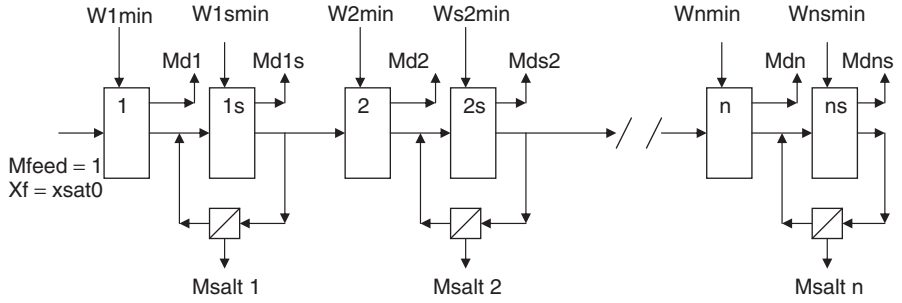

1, 2, n concentrator

1s, 2s,,,,ns crystallizer at xsat

Figure 1.A.1 Theoretical processing of a feed of n salt saturation limits.

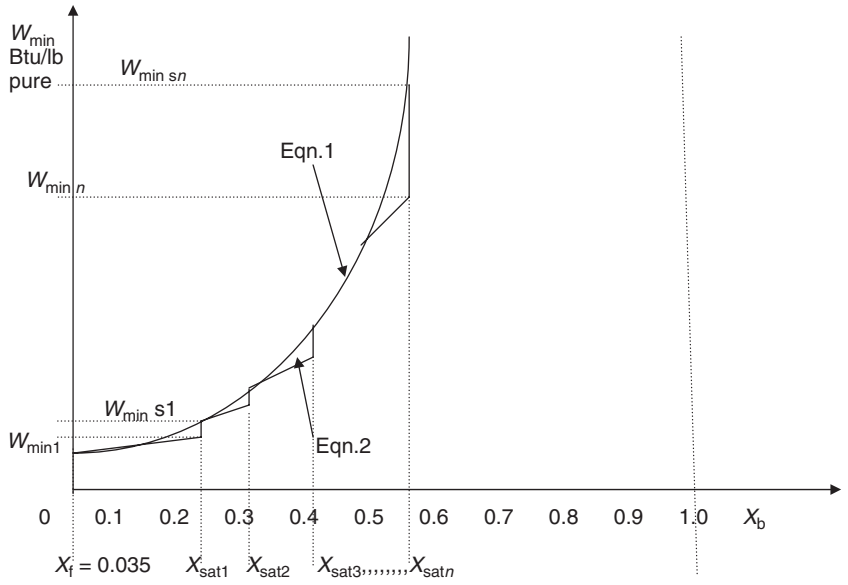

Figure 1.A.2 Feed of n Saturation limits on $w_{theor}-x_{sat}$ coordinates.

sodium chloride aqueous solution as feed. Zero-liquid-discharge desalting is 2 times the conventional seawater theoretical requirement for seawater salt content as feed. It is 3 times the conventional reject brine salt content as feed, and it is 6 times that with oilfield product–water salt content as feed. Without improved desalting efficiency, a similar trend is expected for actual work requirement and for cost since the cost of energy is a major part of the desalination processes. Improved desalting efficiency may be sufficient to justify competitive zero liquid discharge of seawater or its conventional reject brine. For produced water as feed, a net environmental benefit is also needed to justify competitiveness.

The theoretical work described above is derived assuming sodium chloride aqueous solution as an ideal solution. A factor >1 is often used to accommodate the deviation from ideality.

Any saline water contains more than one salt species. Depending on composition and the solubility limits of the individual salts in water, a sequence of precipitations peculiar to the saline water is expected.

Let n be the number of saturation limits occurring one after the other (consecutively), and let the feed be denoted by $x_{sat}(0)$ of $M_d(0) = 0$. The minimum work per unit feed becomes

$$W_{min,fd=1} = \sum_{i=0}^{i=n} M_d(i) RT \frac{x_{sat}(i)\ x_{sat}(i-1)}{x_{sat}(i) - x_{sat}(i-1)} \ln\left[\frac{x_{sat}(i)}{x_{sat}(i-1)}\right] \quad (1.A.43c)$$

where

$$\mathrm{M_d}(i) = \sum_{\mathrm{i=1}}^{i=n-1} \left(1 - M_{\mathrm{d}}(i)\frac{x_{\mathrm{sat}}(i) - x_{\mathrm{sat}}(i-1)}{x_{\mathrm{sat}}(i)}\right) \tag{1.A.44}$$

Figure 1.A.1 shows the theoretical processing of a saline water of n saturation limits by a sequence of concentrators where the work defined by Equation (1.A.42) applies, and for crystallizers where the work by equation (1.A.41a) applies at saturation limits. Figure 1.A.2 shows the same information on work-concentration coordinates.

Please refer to Tables 1.A.4–1.A.7. for selected useful properties

Table 1.A.4 Constant-Pressure Specific Heats of Ideal Gases

Gas	$C_p(\tau)$; $\tau = T\mathrm{K}/100$		Temperature Range, K	Maximum error, %
O_2	$C_{\mathrm{po}} = 37.432 + 0.020102\tau^{1.5}$	$-178.57\tau^{-1.5} + 236.88\tau^{-2}$	300–3500	0.30
N_2	$C_{\mathrm{po}} = 39.060 - 512.79\tau^{1.5}$	$+1072.7\tau^{-2} - 820.40\tau^{-3}$	300–3500	0.43
H_2O	$C_{\mathrm{po}} = 143.05 - 183.54\tau^{0.2.5}$	$+82.75\tau^{0.5} - 3.6989\tau$	300–3500	0.43
CO_2	$C_{\mathrm{po}} = -3.7357 + 30.529\tau^{0.5}$	$-4.1034\tau + 0.024198\tau^2$	300–3500	0.19
CO	$C_{\mathrm{po}} = 69.145 - 0.70463\tau^{0.75}$	$-200.77\tau^{-0.5} + 176.76\tau^{-0.75}$	300–3500	0.42
H_2	$C_{\mathrm{po}} = 56.565 - 702.74\tau^{-0.75}$	$+1165.0\tau^{-1} - 560.7\tau^{-1.5}$	300–3500	0.60
OH	$C_{\mathrm{po}} = 81.546 - 59.35\tau^{0.25}$	$+17.329\tau^{0.75} - 4.2660\tau$	300–3500	0.43
NO	$C_{\mathrm{po}} = 59.283 - 1.7096\tau^{0.5}$	$-70.613\tau^{-0.5} + 74.889\tau^{-1.5}$	300–3500	0.34
NO_2	$C_{\mathrm{po}} = 46.045 + 216.10\tau^{-.5}$	$-363.66\tau^{-0.75} + 232.55\tau^{-2}$	300–3500	0.26
CH_4	$C_{\mathrm{po}} = -672.87 + 439.74\tau^{0.25}$	$-24.875\tau^{07.5} + 323.88\tau^{-0.5}$	300–2000	0.15
C_2H_4	$C_{\mathrm{po}} = -95.395 + 123.15\tau^{0.5}$	$-35.641\tau^{07.5} + 182.77\tau^{-3}$	300–2000	0.07
C_2H_6	$C_{\mathrm{po}} = 6.895 + 17.26\tau$	$-0.6402\tau^2 + 0.00728\tau^3$	300–1500	0.83
C_3H_8	$C_{\mathrm{po}} = -4.042 + 30.46\tau$	$-1.571\tau^2 + 0.03171\tau^3$	300–1500	0.40
C_4H_{10}	$C_{\mathrm{po}} = 3.945 + 37.12\tau$	$-1.833\tau^2 + 0.03498\tau^3$	300–1500	0.54

Table 1.A.5 Critical Constants

Substance	Formula	Molecular Weight	Temprerature, K	Pressure, MPa	Volume, m^3/kmol
Ammonia	NH_3	17.03	405.5	11.28	0.0724
Argon	Ar	39.948	151	4.86	0.0749
Bromine	Br_2	159.808	584	10.34	0.1355
Carbon dioxide	CO_2	44.01	304.2	7.39	0.0943
Carbon monoxide	CO	28.011	133	3.50	0.0930
Chlorine	Cl_2	70.906	417	7.71	0.1242
Deuterium	D_2	4.00	38.4	1.66	—
Helium	He	4.003	5.3	0.23	0.0578
Hydrogen	H_2	2.016	33.3	1.30	0.0649
Krypton	Kr	83.80	209.4	5.50	0.0924
Neon	Ne	20.183	44.5	2.73	0.0417

Table 1.A.5 (*Continued*)

Substance	Formula	Molecular Weight	Temprerature, K	Pressure, MPa	Volume, m^3/kmol
Nitrogen	N_2	28.013	126.2	3.39	0.0899
Nitrous oxide	N_2O	44.013	309.7	7.27	0.0961
Oxygen	O_2	31.999	154.8	5.08	0.0780
Sulfur dioxide	SO_2	64.063	430.7	7.88	0.1217
Water	H_2O	18.015	647.3	22.09	0.0568
Xenon	Xe	131.30	289.8	5.88	0.1188
Benzene	C_6H_6	78.115	562	4.92	0.2603
n-Butane	C_4H_{10}	58.124	425.2	3.80	0.2547
Carbon tetrachloride	CCl_4	153.82	556.4	4.56	0.2759
Chloroform	$CHCl_3$	119.38	536.6	5.47	0.2403
Dichlorodifluoromethane	CCl_2F_2	120.91	384.7	4.01	0.2179
Dichlorofluoromethane	CCl_2F	102.92	451.7	5.17	0.1973
Ethane	C_2H_6	30.070	305.5	4.88	0.1480
Ethyl alcohol	C_2H_5OH	46.070	516	6.38	0.1673
Ethylene	C_2H_4	28.054	282.4	5.12	0.1242
n-Hexane	C_6H_{14}	86.178	507.9	3.03	0.3677
Methane	CH_4	16.043	191.1	4.64	0.0993
Methyl alcohol	CH_3OH	32.042	513.2	7.95	0.1180
Propane	C_3H_8	44.097	370	4.26	0.1998
Propene	C_3H_6	42.081	365	4.62	0.1810
Propyne	C_3H_4	40.065	401	5.35	—
Trichlorofluoromethane	CCl_3F	137.37	471.2	4.38	0.2478

Table 1.A.6 Enthalpy and Gibbs Free Energy of Formation and Absolute Entropy of Some Substances at 25°C and 0.1 MPa

Substance	Formula	Molecular Weight	State	H_f, kJ/kmol	G_f, kJ/.kmol	S, kJ/ (kmol.K)
Carbon monoxide	CO	28.011	gas	−110,529	−137,150	197.653
Carbon dioxide	CO_2	44.011	gas	−393,522	−394,374	213.795
Water	H_2O	18.015	gas	−241,827	−228,583	188.833
Water	H_2O	18,015	liquid	−285,838	−237,178	70.049
Methane	CH_4	16.043	gas	−74,873	−50,751	186.256
Acetylene	C_2H_2	26.038	gas	+226,731	+209,234	200.958
Ethene	C_2H_4	28.054	gas	+52,283	+68,207	219.548
Ethane	C_2H_6	30.070	gas	−84,667	−32,777	229.602
Propane	C_3H_8	44.097	gas	−103,847	−23,316	270.019
Butane	C_4H_{10}	58.124	gas	−126,148	−16,914	310.227
Octane	C_8H_{18}	114.23	gas	−208,447	+16,859	466.835
Octane	C_8H_{18}	114.23	liquid	−249,952	+6,940	360.896
Carbon (graphite)	C	12.011	solid	0	0	5.795

Table 1.A.7 Logarithms to Base e of the Equilibrium Constant K[a]

T, K	$H_2 = 2H$	$O_2 = 2O$	$N_2 = 2N$	$H_2O = H_2 + 0.5O_2$	$H_2O = 0.5H_2 + OH$	$CO_2 = CO + 0.5O_2$	$0.5N_2 + 0.5O_2 = NO$
298	−164.005	−186.975	−367.480	−92.208	−106.208	−103.762	−35.052
500	−92.827	−105.630	−213.372	−52.691	−60.281	−57.616	−20.295
1000	−39.803	−45.150	−99.127	−23.163	−26.034	−23.529	−9.388
1200	−30.874	−35.005	−80.011	−18.182	−20.283	−17.871	−7.569
1400	−24.463	−27.742	−66.329	−14.609	−16.099	−13.842	−6.270
1600	−19.837	−22.285	−56.055	−11.921	−13.066	−10.830	−5.294
1800	−15.866	−18.030	−48.051	−9.826	−10.657	−8.497	−4.536
2000	−12.840	−14.622	−41.645	−8.145	−8.728	−6.635	−3.931
2200	−10.353	−11.827	−36.391	−6.768	−7.148	−5.120	−3.433
2400	−8.276	−9.497	−32.011	−5.619	−5.832	−3.860	−3.019
2600	−6.517	−7.521	−28.304	−4.648	−4.719	−2.801	−2.671
2800	−5.002	−5.826	−25.117	−3.812	−3.763	−1.894	−2.372
3000	−3.685	−4.357	−22.359	−3.086	−2.937	−1.111	−2.114
3200	−2.534	−3.072	−19.937	−2.451	−2.212	−0.429	−1.888
3400	−1.516	−1.935	−17.800	−1.891	−1.576	0.169	−1.690
3600	−0.609	−0.926	−15.898	−1.392	−1.088	0.701	−1.513
3800	0.202	−0.019	−14.199	−0.945	−0.501	1.176	−1.356
4000	0.934	0.796	−12.660	−0.542	−0.044	1.599	−1.216
4500	2.486	2.513	−9.414	0.312	0.920	2.490	−0.921
5000	3.725	3.895	−6.807	0.996	1.689	3.197	−0.686
5500	4.743	5.023	−4.666	1.560	2.318	3.771	−0.497
6000	5.590	5.963	−2.865	2.032	2.843	4.245	−0.341

[a] For the reaction $n_aA + n_bB = n_cC + n_dD$, the equilibrium constant is defined as $K = ({a_C}^{nc}{a_D}^{nd})/({a_A}^{na}{a_B}^{nb})$.

Symbols (some additional symbols definitions are in the text where they are mentioned, and in the associated software)

A	membrane water permeability coefficient lb/(h · ft^2· psi) [or m/(h.bar)]; surface area, A_{min} surface area minimized by design degrees of freedom
B	membrane salt permeation coefficient ft/h (or m/h)
c	salt concentration per unit volume, lb/ft^3 (or kg/m^3); c_b of bulk; c_m of high-pressure-side membrane wall; c_d of diluted product
c_d	unit cost of exergy destruction \$/kWh, c_{da}, system average
C_a	cost per unit characterizing surface (area)
C_{aED}	cost per unit surface of ion exchange electrodialysis membranes
C_{aPV}	solar cell module cost per unit surface
C°_{aPV}	solar cell module cost per unit surface under standard test conditions
C_{aRO}	cost per unit membrane surface under reverse-osmosis (R conditions)
C_f	fuel price per kWh exergy
C_F	fuel price per kWh higher heating value
C_{pwr}	unit power cost, \$/kWh
C_{wtr}	production cost per unit product, \$/m^3

C_z	capital recovery rate \$/\$·y: $C_{z\mathrm{M}}$ for membranes, $C_{z\mathrm{RO}}$ for remaining RO devices, $C_{z\mathrm{PV}}$ for solar cells
Cap	capital cost, Cap^{+}, added capital
d	Diameter or equivalent diameter, ft
D	diffusion coefficient, m^2/s; dissipation, kW (exergy destruction rate)
$D^{\mathrm{th}}10$	temperature difference in the condenser, F
E	exergy; E^{s}, of system; E^{f}, of flow
f	friction factor
F	fuel; F_{penalty} for fuel penalty, F_{idealc} for fuel of ideal control, $\mathrm{Np}_{\mathrm{fuel}}$ for fuel of night product, F_{refired} for fuel of refiring
F_{ms}	PV cost multiplier accounting for added cost from module to system
h_{m}	RO mass transfer coefficient, ft/h (or m/h)
hhv	fuel higher heating value
H	enthalpy; height of flow passage, in. (or mm); H_{b}, of RO membrane feed side; H_{d}, of its product low-pressure, side; $H_{\mathrm{hc}}, H_{\mathrm{lc}}$, osmosis high- and low-concentration sides, respectively
J	objective function, \$/h; mass flux, $\mathrm{lb/(h{\cdot}ft^2)}$ [or $\mathrm{kg/(h \cdot m^2)}$] J_{w}, of pure water; J_{s} of salt; J_{v}, volume flux, ft/h (or m/h)
LF	power load factor
mgd	million gallons per day; migpd, Imperial; usmgd, American
M_{d}	PV/RO water product rate usmgd (m^3/d)
N	dimensionless number; N_{V}, velocity/geometry number; N_{M}, a membrane number [Eq. 4.24]
OP	variable-load operation, $\mathrm{OP}_{\mathrm{pen}}$, operation cost penalty
P	Applied pressure, psia (or bar); P_0, dead-state pressure
P_{w}	Power, kW; P_{load}, power required; P_{dlvrd}, power delivered
ppm	RO product water salt content, parts per million; ED feed parts per million
P_{zn}	RO concentration polarization ratio $x_{\mathrm{sm}}/x_{\mathrm{sb}}$ (salt at membrane wall/bulk)
R	universal gas constant; resources, R_{manuf}, manufacturing resources of a device, R_{operate} operating resources of a device
R_{eff}	Ratio of PV expected solar cell field efficiency to standard test conditions top cell efficiency η/η°
R_{sol}	the ratio of design solar intensity to the standard test intensity sol/sol°
S	entropy
S_{PV}	solar cell surface, m^2; S°_{PV}, of standard test conditions
S_{RO}	RO membrane surface, m^2
Sol	design solar intensity, $\mathrm{kW/m^2}$; Sol°: of standard test conditions ($1\mathrm{kW/m^2} = 1$ sun)
T	temperature; T_o dead-state temperature
V	device decision variables, $V_{\mathrm{efficiency}}$, thermodynamic; V_{design} design $V_{\mathrm{manufacture}}$ manufacture
X	dependent variable, X_{duty}, for a device

x_s	Salt mass fraction; x_{sf}, of feed, x_{sj}, of reject brine; x_{sm}, at membrane wall; x_{sb}, of bulk flow; x_{sd}, of product water
Z	capital cost, \$; Z_{RO}, for RO subsystem; Z_{PV}, for PV module; Z_{PVS} for solar subsystem; Z_{VC}, for VC subsystem; Z_{ED}, for electrodialysis subsystem; Z_{GT}, for gas turbine subsystem; Z_{MSF}, multistage flash distillation subsystem
$\mathbf{Z}$	capital cost rate
δ	concentration boundary-layer thickness, μm (10^{-6}m)
ΔP_h	pressure loss, psi (or kPa), high-pressure side of RO membrane
ϕ	departure from ideal solution; 1 for ideal solution; ϕ_P, of RO applied pressure
η	efficiency; η_{RO}, of separation process; η_{PV}, of solar-to-power conversion; $\eta^o{}_{PV}$, of standard test conditions; η_{pmp}, adiabatic efficiency of pressurizing pump; η_{trb}, adiabatic efficiency of work recovery turbine or device
ρ	density
μ	viscosity; chemical potential; μ_{c0}, chemical potential of species at dead state P_0 and T_0

Abbreviations

ED	electrodialysis desalter
EL	water electrolysis system
GT/MSF	gas turbine/multistage flash distillation cogeneration system
PV	photovoltaic (solar cells)
RO	reverse-osmosis desalter
SCC	simple combined cycle
VC	vapor compression (distiller)
ZLD	zero liquid discharge

SELECTED REFERENCES FOR SECTION 1.1–1.3

1. Tribus M, Evans R, *The Thermoeconomics of Sea Water Conversion*, UCLA Report 62–63, Aug. 1962.
2. El-Sayed Y, Evans R, Thermoeconomics and the design of heat systems, *J. Eng. Power* 27–35 (Jan. 1970).
3. El-Sayed Y, Aplenc A, Application of the thermoeconomic approach to the analysis and optimization of a vapor-compression desalting system, *J. Eng. Power* 17–26 (Jan. 1970).
4. Gaggioli R, ed., *Thermodynamics: Second Law Analysis*, ACS Symp. Series 122, *American Chemical Society*, 1980.
5. Gaggioli R, ed., *Efficiency and Costing*, ACS Symp. Series 235, 1983.
6. El-Sayed Y, A second-law-based optimization, Parts 1 and 2, *J. Eng. Gas Turb. Power* **118**:693–703 (Oct. 1996).

7. Torres C, Serra L, Valero A, Lozano M, The productive structure and thermoeconomic theories of system optimization, *Proc. ASME Adv. Energy Syst. Div*. **36**:429–436 (Nov. 1996).
8. Lazaretto A, Tsatsaronis G, On the quest for objective equations in exergy costing, *Proc. ASME*. **37**:197–210 (1997).
9. Linhoff B, The use of pinch analysis to knock down capital costs and emissions, *Chem. Eng. Progress*, 32–57 (Aug. 1994).
10. Sciubba E, Melli R, *Artificial Intelligence in Thermal Systems Design*, Nova Scientific Publishers, 1998.
11. Dimopoulos GG, Christos A, Frangopoulos CA, Optimization of energy systems based on evolutionary and social metaphors, *Energy* **33**:171–179 (2008).
12. Bouvy C, Lucas K, Multicriterial optimization of communal energy supply concepts, *Proc. 19th Int. ECOS Conf*., Greece, 2006, Vol. 1, pp. 543–551.
13. Gibbs JW, (1978), *On the Equilibrium of Heterogeneous Substances, The Collected Work*, Yale Univ. Press, 1978, (orig. publ. 1928, Vol. 1, p. 77).
14. El-Sayed Y, *The Thermoeconomics of Energy Conversions*, Elsevier (UK), 2003.
15. El-Sayed YM, The rising potential of competitive solar desalination, *Desalination* **216**:314–324 (2007).
16. Baker RW, *Membrane Technology and Applications*. Wiley, Hoboken, NJ, 2004.
17. Reid R, Pruasnitz J, Poling B, *The Properties of Gases and Liquids*, 4th ed., McGraw-Hill, 1989.
18. Green MA, *Third Generation of Photovoltaics, Advanced Solar Energy Conversion* Springer-Verlag, 2003.
19. Mulder M, *Basic Principles of Membrane Technology*, Kluwer Academic, 2003.
20. Sehra A, Bettner J, Cohen A, Design of a high performance axial compressor for utility gas turbines, *J. Turbomach*. 114(2):277–286 (1992).
21. Cohen H, Rogers G, Saravenamuttoo H, *Gas Turbine Theory*, 3rd ed., Wiley, 1987.
22. Hegetschweiler H, Bartlet R, Predicting performance of large steam turbine-generator units, *Trans. Am. Soc. Mech. Eng. ASME.* 79:1085–1114 (1957).
23. Sabersky R, Acosta A, Hauptmann E, *Fluid Flow, a First Course in Fluid Mechanics*, 3rd ed., Macmillan, 1989.

FURTHER READING

1.F.1 International Symposia on Energy Analysis

Pleskov YV, *Solar Energy Conversion: A Photoelectrochemical Approach*, Springer-Verlag, 1992.

Luque A, Hegedus S, ed., *Handbook of Photovoltaic Science and Engineering*, Wiley, Hoboken, NJ, 2003.

Moran M, Sciubba E, eds., *Proc. 4th Int. Symp. Second Law Analysis of Thermal Systems*, Rome, May 25–29, 1987.

Cai, Ruixian, Moran M, eds., *Proc. Int. Symp. Thermodynamic Analysis and Improvement of Energy Systems*, (TAIES'89), Beijing, June 5–8, 1989.

Stecco S, Moran M, eds., *Proc. Florence World Energy Research Symp*. (FLOWERS'90), Florence, Italy, May 28–June 1, 1990.

Proc. Int. Conf. Analysis of Thermal and Energy Systems (Athens'91), Athens, 1991.

Valero A, Tsatsaronis G, editors: *Proc. Int. Symp. Efficiency, Costs, Optimization, and Simulation of Energy Systems* (ECOS'92), Zaragoza, Spain, June 15–18, 1992.

Proc. Int. Symp. Energy Systems and Ecology (Ensec'93), Krakow, Poland, July 5–9, 1994.

Proc. Florence World Energy Research Symp. (FLOWERS'94), Florence, July 6–8, 1994.

Proc. Int. Symp. Efficiency, Costs, Optimization, Simulation and Environmental Impact of Energy Systems (ECOS'95), Istanbul, July 9–14, 1995.

Proc. Int. Symp. Efficiency, Costs, Optimization, Simulation and Environmental Impact of Energy Systems (ECOS'96), Stockholm, June 25–27, 1996.

Proc. Int. Symp. Thermodynamic Analysis and Improvement of Energy Systems, (TAIES'97), Beijing, June 10–13, 1997.

Proc. Int. Symp. Efficiency, Costs, Optimization, Simulation and Environmental Aspects of Energy Systems and Processes (ECOS'98), Nancy, France, July 8–10, 1998.

Proc. Int. Symp. Efficiency, Costs, Optimization, Simulation and Environmental Aspects of Energy Systems (ECOS'99), Tokyo, June 8–10, 1999.

Proc. Int. Symp. Efficiency, Costs, Optimization, and Simulation of Energy Systems (ECOS'00), Univ. Twente, The Netherlands, July 5–7 2000.

Proc. Int. Symp. Efficiency, Costs, Optimization, Simulation and Environmental Impact of Energy Systems (ECOS'01), Istanbul, July 4–6, 2001.

Proc. Int. Symp. Efficiency, Costs, Optimization, and Simulation of Energy Systems (ECOS'02), Berlin, July 3–5, 2002.

Proc. Int. Symp. Efficiency, Costs, Optimization, and Simulation of Energy Systems (ECOS'03), Denmark, June 30–July 2, 2003.

Proc. 17th Int. Conf. Efficiency, Cost, Optimization, Simulation and Environmental Impact of Energy and Process Systems (ECOS'2004), Guanajauto, Mexico, July 7–9, 2004.

Proc. 18th Int. Conf. Efficiency, Cost, Optimization, Simulation and Environmental Impact of Energy Systems (ECOS'2005), Trondheim, Norway, June 20–22, 2005.

Proc. 19th Int. Conf. Efficiency, Cost, Optimization, Simulation and Environmental Impact of Energy Systems (ECOS'2006), Aghia Pelagia, Crete, Greece, July 12–14, 2006.

Proc. 20th Int. Conf. Efficiency, Cost, Optimization, Simulation and Environmental Impact of Energy Systems (ECOS'2008), Krakow Gliwicw, Poland, June 24–27, 2008.

The 22nd International Conference on Efficiency, Cost, Optimization, Simulation and Environmental Impact of Energy Systems (ECOS'2009) held in Foz do Iguaçú, Brazil, 31 August -- 3 September 2009.

The 23rd International Conference on Efficiency, Cost, Optimization, Simulation and Environmental Impact of Energy Systems (ECOS'2010) held in Lausanne, Switzerland, 14-17 June 2010.

The 24th International Conference on Efficiency, Cost, Optimization, Simulation and Environmental Impact of Energy Systems (ECOS'2011) held in Novi Sad, Serbia, 4-7 July 2011.

1.F.2 Selected International Symposia on Desalination

Proc. IDA World Congress Desalination and Water Sciences, Abu Dhabi, UAE, Nov. 18–24, 1995.

Proc. IDA World Congress Desalination and Water Reuse, Madrid, Oct. 6–9, 1997.

Proc. European Conf. Desalination and the Environment, Las Palmas, Gran Canaria, 1999.

Proc. The Int. Conf. Seawater Desalination Technologies on the Threshold of the New Millennium, Kuwait, Nov. 4–7, 2000.

Proc. IDA Int. Conference Desalination, Singapore, March 21–22, 2001.

Proc. IDA World Congress Desalination and Water Reuse, Bahrain, March 8–13, 2002.

Proc. IDA World Congress Desalination, and Water Reuse, Paradise Island, Bahamas, Sept. 28–Oct. 3, 2003.

Proc. Int. Conf. Water Security for Future Generations,, Changchun, Jilin Province, China, July 26–31, 2004.

Proc. IDA World Congress Desalination and Water Reuse, Singapore, Sept. 11–16, 2005.

Proc. ADST 2006 Int. Conf. Desalination Technologies and Water Reuse, Alexandria, Egypt, May 6–8, 2006.

Proc. AMTA Membrane Technologies Conf., Las Vegas, NV (USA), July 23–26, 2007.

Proc. IDA World Congress Desalination and Water Reuse, Maspalomas, Gran Canaria, Spain, Oct. 21–26, 2007.

IDA World Congress on Desalination and water Reuse, Dubai, November 7-12, 2009.

IDA World Congress on Desalination and water Reuse, Perth, Australia, September 4-9, 2011.

1.F.3 Books on Thermodynamics

Gaggioli RA, ed., *Thermodynamics: Second Law Analysis*, ACS Symp. Series Vol. 122, American Chemical Society, 1980.

Moran MJ, *Availability Analysis, A Guide to Efficient Energy Use*, Prentice Hall, 1982.

Kotas TJ, *The Exergy Method of Thermal Plant Analysis*, Butterworth, 1984.

Reid R, Pruasnitz J, Poling B, *The Properties of Gases and Liquids*, 4th ed., McGraw-Hill, 1989.

Szargut J, Morris D, Steward F, *Exergy Analysis of Thermal, Chemical and Metallurgical Processes*, Hemisphere Publishing, 1985.

Van Wylen GJ, Sonntag RE, *Fundamentals of Classical Thermodynamics*, Wiley 1996.

1.F.4 Books on Optimization and Equation Solvers

Wilde DJ, Beightler CS, *Foundations of Optimization*, Prentice-Hall, 1967.

Intriligator M, *Mathematical Optimization and Economic Theory*, Prentice-Hall, 1971.

Wismer D, Chattergy R, *Introduction to Nonlinear Optimization, a Problem Solving Approach*, North-Holland Series in System Science and Engineering, 1978.

Chapra S, Canale R, *Numerical Methods for Engineers*, 2nd ed., McGraw-Hill, 1988.

1.F.5 Books on Design of Energy Conversion Devices

Hottel H, Sarofim A, *Radiative Transfer*, McGraw-Hill, 1967.

Siegel R, Howell J, *Thermal Radiation Heat Transfer*, 2nd ed., Hemisphere Publishing, 1981.

Rohsenow W, Hartnett J, Ganic E, *Handbook of Heat Transfer Applications*, 2nd ed., McGraw Hill Book Company.

Cohen H, Rogers G, Saravenamuttoo H, *Gas Turbine Theory*, 3rd ed., Wiley, 1987.

Sabersky R, Acosta A, Hauptmann E, *Fluid Flow, a First Course in Fluid Mechanics*, 3rd ed., Macmillan, 1989.

1.F.6 Books on Optimal Design

Edgerton R, *Available Energy and Environmental Economics*, Lexington Books.

Gaggioli R, ed., *Efficiency and Costing*, ACS Symp. Series Vol. 235, American Chemical Society, 1983.

Papalambros PY, Wilde DJ, *Principles of Optimal Design, Modeling and Computation*, Cambridge Univ. Press, 1988.

Edger TF, Himmelblau DM, *Optimization of Chemical Processes*, McGraw-Hill, 1988.

Bejan A, Tsatsaronis G, Moran M, *Thermal Design and Optimization*, Wiley, 1996.

El-Sayed YM, *The Thermoeconomics of Energy Conversions*, Elsevier, 2003.

1.F.7 Books on Emerging Technologies (Fuel/Solar Cells and Selective Membranes)

Kordesch K, Simader G, *Fuel Cells and Their Applications*, VCH, 1996.

Minh NQ, Takahashi T, *Science and Technology of Ceramic Fuel Cells*, Elsevier, 1995.

Appleby AJ, ed., *Fuel Cells: Trends in Research and Applications*, Hemisphere Publishing, 1987.

Mazer JA, *Solar Cells: An Introduction to Crystalline Photovoltaic Technology*, Kluwer Academic, 1997.

Pleskov YV, *Solar Energy Conversion: A Photoelectrochemical Approach*, Springer-Verlag, 1990.

Mulder M, *Basic Principles of Membrane Technology*, 2nd ed., Kluwer Academic 1996.

Baker RW, *Membrane Technology and Applications*, Wiley, 2004.

Luque A, Hegedus S, eds., *Handbook of Photovoltaic Science and Engineering*, Hegedus, editors, Wiley, 2003.

Green MA, *Third Generation Photovoltaics, Advanced Solar Energy Conversion*, Springer, 2003.

1.F.8 General Additional Reading for Section 1.2

Bejan A, Tsatsaronis G, Moran M, *Thermal Design and Optimization*, Wiley, 1996.

Chapra SC, Canale RP, *Numerical Methods for Engineers*, McGraw-Hill, 1988.

DeGarmo E, Sullivan W, Bontadelli J, Engineering Economy, 9th ed., Macmillan, 1992.

Dunbar WR, Lior N, Gaggioli R, Combining fuel cells with fuel-fired power plants for improved exergy efficiency, *Energy* 16:(10)1259–1274 (1991).

Dunbar WR, Lior N, Gaggioli R, The component equations of energy and exergy, *ASME J. Energy Resources Technol*. 114:75–83 (1992).

Dunbar WR, Lior N, Gaggioli R, The effect of the fuel-cell unit size on the efficiency of a fuel-cell-topped Rankine Cycle, *ASME J. Energy Resources Technol*. 115:105–107 (1993).

Dunbar WR, Lior N, Sources of combustion irreversibility, *Comb. Sci. Technol*. 103:41–6 (1994).

Edger TF, Himmelblau DM, *Optimization of Chemical Processes*, McGraw-Hill, 1988.

Edgerton R, *Available Energy and Environmental Economics*, Lexington Books, 1982.

Evans RB, *A Proof that Essergy is the Only Consistent Measure of Potential Work*, PhD thesis, Thayer School of Engineering, Dartmouth College, Hanover, NH, 1969.

Incropera F, DeWitt D, Fundamentals of Heat and Mass Transfer, 3rd ed., Wiley, 1990.

Keenan JH, *Thermodynamics*, Wiley, 1941.

Kotas TJ, *The Exergy Method of Thermal Plant Analysis*, Butterworth, 1984.

Lior N, Sarmiento-Darkin W, Al-Sharqawi HS, The exergy fields in transport processes: Their calculation and use, *Energy* 31:553–578 (2006).

Means RS, *Mechanical, Building, and Electrical Cost Data*, Construction Publishers and Consultants, Kingston, MA, 1998.

Modern Cost Engineering: Methods and Data, compiled by *Chemical Engineering*, McGraw-Hill, 1979.

Moran MJ, *Availability Analysis, A Guide to Efficient Energy Use*, Prentice-Hall, 1982.

Papalambros PY, Wilde DJ, *Principles of Optimal Design, Modeling and Computation*, Cambridge Univ. Press, 1988.

Rant Z, Exergie, ein neues wort fur technische arbeitsfahigkeit, *Forsch. Ing. Wissen*. **22**(1):25–32 (1956).

Szargut J, Morris D, Steward F, *Exergy Analysis of Thermal, Chemical and Metallurgical Processes*, Hemisphere Publishing, 1985.

Van Wylen RE, Sonntag GJ, *Fundamentals of Classical Thermodynamics*, Wiley, 1996.

Wilde DJ, Beightler CS, *Foundations of Optimization*, Prentice-Hall 1967.

1.F.9 General Additional Reading for Section 1.4

Archer Enterprises, *Report on the Commercial Electrolytic Production of Hydrogen*, Geneva, NY.

Darwish MA, Al-Najem NM, Lior N, Towards sustainable seawater desalting in the Gulf area, *Desalination* Vol. 235, 5887, (2009).

Echeverria A, Desalination plant in Tenerife, San Loranzo Valley, *Proc. IDA World Congress Desalination and Water Reuse*, Madrid, Oct. 6–9, 1997, Vol. II, pp. 675–694.

El-Nashar AM, Validating the simulation program "Soldes" with actual performance data from an operating solar desalination plant, *Proc. IDA World Congress Desalination and Water Reuse*, Madrid, Oct. 6–9, 1997, Vol. 1, pp. 107–142.

El-Sayed YM, Desirable enforcements to optimal system design, *Proc. 19th Int. Conf. Efficiency, Cost, Optimization, Simulation and Environmental Impact of Energy Systems* (ECOS'06), Aghia Pelagia, Crete, Greece, July 12–14, 2006, Vol. 1, pp. 483–492.

Maloney K, Dopp R, *Highly Efficient Hydrogen Generation via Water Electrolysis Using Nanometal Electrodes*, Energy Research Laboratory, QuantumSphere Inc., Santa Ana, CA.

Torres del Corral M, (del) Pino, MP, Lodos MG, Rodrigous M, Physico-chemical and electrodialysis reversal treatment to reclaim wastewater from a sewage treatment plant, Proce. IDA World Congress Desalination and Water Reuse, Madrid, Oct. 6–9, 1997, Vol. II, pp. 695–711.

Van Wylen RE, Sonntag GJ, *Fundamentals of Classical Thermodynamics*, Wiley, 1996.

Yongqing Wang, Noam Lior, Fuel allocation in a combined steam-injected gas turbine and thermal seawater desalination system, *Desalination* Vol. 214, 306326, (2007).

1.F.10 Literature on Design Models

El-Sayed Y, On the feasibility of large vapor compression distillation units, *Desalination* 107:13–27, (1996).

El-Sayed Y, On the development of large vapor compression distillation units, *Proc. Int. Desalination Assoc. Desalination Seminar*, Cairo, Sept. 6–8, 1997.

El-Sayed Y, Gaggioli R, The integration of synthesis and optimization for conceptual designs of energy systems, *J. Energy Resources Technol*. 110:109–113 (1988).

Hoyt H, Sarofim A, *Radiative Transfer*, McGraw-Hill, 1967.

Rohsenow W, Hartnett J, Ganic E, *Handbook of Heat Transfer Applications*, 2nd ed., McGraw-Hill, (1985).

Siegel R, and Howell J, *Thermal Radiation Heat Transfer*, 2nd ed., Hemisphere Publishing, 1981.